Table 1
Clinical, allergological and MRI findings of patients with juvenile muscular atrophy of distal upper extremity

	Patient no.										
	1	2	3	4	5	6	7	8	9	10	11
Age at onset (years)	12	13	15	16	17	18	15	18	17	17	16
Age at examination (years)	13	15	22	17	19	19	15	20	20	22	19
Sex	F	F	M	M	M	M	M	M	M	M	M
Onset mode	Insidious	Insidious	Insidious	Insidious	Insidious	Insidious	Insidious	Insidious	Insidious	Insidious	Insidious
Muscle atrophy of distal upper extremity	R>L	R>L	R<L	R	R>L	R<L	R	R	R>L	R<L	R
Coexisting atopic/allergic disorders											
Bronchial asthma	+[a]	–	–	(+)[b]	–	–	–	–	–	–	(+)[b]
Allergic rhinitis	–	+	+	+	–	+	+	–	–	–	+
Pollinosis	–	–	+	–	–	–	–	+	+	+	+
Atopic dermatitis	–	–	–	–	–	–	(+)[b]	–	–	–	–
Others	+	–	–	–	–	+	+	+	+	+	–
Family history of atopic/allergic disorders	+	+	+	+	+	+	+	–	–	+	+
Peripheral blood eosinophil (%)[c]	7.8	7.6	2.7	4.5	6.7	5.2	5.3	4.4	14.2	2.0	8.3
Total serum IgE (IU/ml)	1874	1225	204	2400	150	220	242	<50	111	324	383
Allergen specific IgE (IU/ml)											
D. pteronyssinus	85.96	>100	9.19	>100	1.52	>100	6.75	–	–	–	44.02
D. farinae	90.66	>100	7.75	>100	2.63	>100	2.78	–	–	–	20.48
Cedar pollen	–	1.53	54.68	0.52	–	2.41	–	0.75	60.13	10.69	0.45
Soya bean	–	–	0.38	NE	–	–	–	–	1.19	0.45	–
Others	–	–	–	NE	–	–	–	–	Rice; 1.32	Wheat; 1.81	Wheat; 0.51
CSF cell count (/μl)	1	NE	NE	NE	NE	0	2	0	0	NE	0
CSF protein (mg/dl)	19	NE	NE	NE	NE	34	32	21	20	NE	17
Cervical MRI on flexion											
Cord flattening	+	+	+	+	+	+	+	+	+	+	–
Epidural venous dilatation	+	+	+	+	+	–	+	–	–	–	–

NE=not examined.
[a] Neurological symptoms developed gradually and were not related to asthma attacks.
[b] History of atopic/allergic disorders not present at the time of neurological illness is shown in parentheses.
[c] Eosinophil percentage higher than 4% is considered hypereosinophilia.

3.2. History of allergic disorders

The frequency of coexisting allergic disorders was significantly higher in patients with JMADUE than in the healthy control subjects (10/11 vs. 11/42, p=0.0002) (Fig. 1A). Of the patients, six (54.5%) had allergic rhinitis and five (45.5%) had pollinosis (Table 1), while in the normal control subjects, five (11.9%) had allergic rhinitis and three (7.1%) had pollinosis. The JMADUE group showed a significantly higher incidence of allergic rhinitis (p=0.0057) (Fig. 1B) and pollinosis (p=0.0064) (Fig. 1C). Two patients (patients 4 and 11) had a history of bronchial asthma that was not present at the time of their neurological illness. Although patient 1 had coexisting bronchial asthma when she developed JMADUE, the neurological symptoms developed gradually and were not related to the asthma attacks. None of the patients had coexisting atopic dermatitis but one (patient 7) had a history of atopic dermatitis that was not present at the time of their neurological illness. Nine of the eleven patients (81.8%) had a family history of allergic disorders in close relatives, and the frequency of a family history of allergic disorders was significantly greater in patients with JMADUE than in control subjects (5/42 (11.9%); p=0.0075) (Fig. 1D).

3.3. Allergological findings

Nine of the eleven patients (81.8%) showed mild to moderate eosinophilia (range 4.4% to 14.2%, normal<4.0%) in peripheral blood (Table 1). HyperIgEaemia was evident in five patients (45.5%), but the frequency of hyperIgEaemia was not significantly different between the patients with JMADUE and control subjects (12/42 (28.6%), p>0.1). All 11 patients had IgE specific for certain common allergens; 8 had IgE specific for two mite antigens, and 8 had IgE specific for cedar pollen. The frequency of mite antigen specific IgE was significantly higher in patients with JMADUE than in the control subjects (*D. pteronyssinus*, 8/11 vs. 14/42, p=0.0361; *D. farinae*, 8/11 vs. 14/42, p=0.0361) (Fig. 1E and F), but the frequency of cedar pollen specific IgE was not significantly different between the two groups (8/11 vs. 27/42, p>0.1).

3.4. Flow cytometric findings

The percentage of intracellular IFNγ^+IL-4$^-$CD4$^+$T cells in peripheral blood did not significantly differ between patients with JMADUE and control subjects (15.5±5.13 vs. 16.9±4.57) (Fig. 2A). The percentage of intracellular

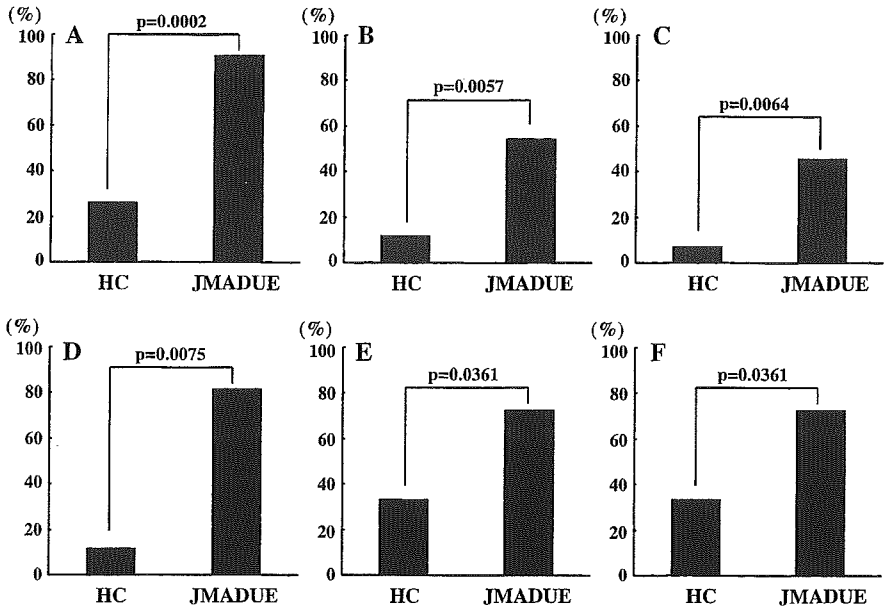

Fig. 1. Allergological features of juvenile muscular atrophy of the distal upper extremity. The frequencies of coexisting allergic disorders are shown: (A) total allergic disorders, (B) allergic rhinitis, (C) pollinosis, and a family history of allergic disorders (D). The frequency of mite antigen specific IgE is shown: (E) *D. pteronyssinus*, (F) *D. farinae*. The ordinate shows frequency in percentage. HC=healthy control subjects, JMADUE=juvenile muscular atrophy of the distal upper extremity.

$IFN\gamma^-IL\text{-}4^+CD4^+$T cells was significantly higher (2.73± 0.32 vs. 2.02±0.68, p=0.0017) (Fig. 2B) in patients with JMADUE compared to control subjects, and hence the intracellular IFNγ/IL-4 ratio in $CD4^+$T cells was significantly reduced (5.67±1.82 vs. 8.92±2.95, p=0.002) (Fig. 2C). There was no significant change in the percentages of either $IFN\gamma^+IL\text{-}4^-$ or $IFN\gamma^-IL\text{-}4^+CD8^+$T cells between the two groups. Neither $IL\text{-}5^+$ nor $IL\text{-}13^+$ cell percentages showed any significant changes between the two groups in either $CD4^+$ or $CD8^+$T cell fractions.

4. Discussion

This is the first flow cytometric study of JMADUE to show a Th2 shift in the immune balance. Moreover, the present study on a greater scale confirmed a previous observation that the frequency of coexisting airway allergies such as allergic rhinitis and pollinosis, a family history of allergic disorders, and mite antigen specific IgE was significantly higher in patients with JMADUE compared to healthy control subjects and indicated a

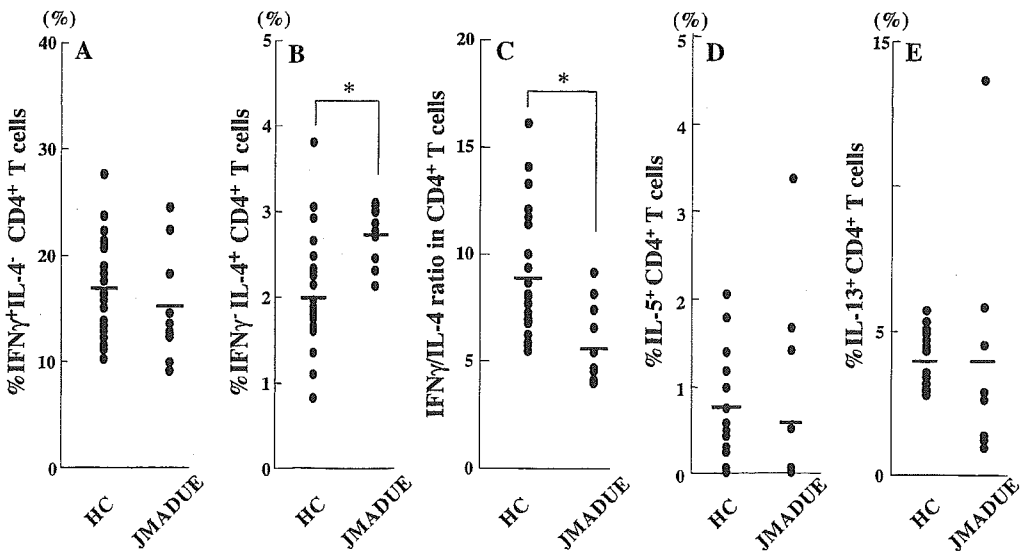

Fig. 2. Analysis of $CD4^+$T cell intracellular cytokine levels. The percentages of $IFN\gamma^+IL\text{-}4^-$ cells (A) and $IFN\gamma^-IL\text{-}4^+$ cells (B), IFNγ/IL-4 ratio (C) and the percentages of $IL\text{-}5^+$ cells (D) and $IL\text{-}13^+$ cells (E) in peripheral blood $CD4^+$T cells. *Statistically significant compared to healthy controls (p<0.01). The number of healthy controls in IL-5 and IL-13 assays is 16. HC=healthy control subjects, JMADUE=juvenile muscular atrophy of the distal upper extremity.

close association between atopic diathesis and JMADUE [4].

In this series, all patients displayed typical clinical features of JMADUE. Based on the radiological and neuropathological findings, repeated dynamic compression of the lower cervical cord followed by circulatory deficiencies may induce damage to the anterior horn cells, which are very vulnerable to ischemia [2,3]. However, neuroimaging showed that only 6 of the 11 patients exhibited flexion myelopathy, cervical cord flattening and epidural venous dilatation. Four patients showed mild cord flattening alone, and another had neither cord flattening nor forward displacement of the cervical dural sac. Other investigators have also failed to detect specific features of flexion myelopathy in some cases with this condition [9,10]. Furthermore, several investigators claim that such a forward displacement of the dural sac, and cord compression with neck flexion are even observed in normal people [9,11]. These findings indicate that JMADUE may be etiologically heterogeneous and that another mechanism other than flexion myelopathy may operate.

In the present study, we provide the first evidence of increases in the percentage of $IFN\gamma^{-}IL\text{-}4^{+}CD4^{+}T$ cells, and a reduction in the intracellular IFNγ/IL-4 ratio in $CD4^{+}T$ cells in JMADUE. Such a Th2 shift is consistent with hypereosinophilia and a heightened IgE response, which are frequently observed in this condition. It is well known that asthmatic amyotrophy (Hopkins syndrome), in which spinal motor neurons are affected, is also associated with atopic diathesis [12,13]. Thus airway allergy and related Th2 shift appear to contribute to cell damage of the spinal anterior horn of young people. On the other hand, we have reported occurrences of myelitis in patients with atopic dermatitis [14–16], naming it atopic myelitis. In this condition, the posterior column is preferentially involved. Although both JMADUE and atopic myelitis affect the cervical cord, involved sites on the axial plane of the spinal cord are distinct, i.e., anterior horns and posterior column, respectively. Therefore, both are considered to be distinct disease entities, yet both commonly have an allergic tendency and Th2 shift. It is interesting to note that atopic myelitis is preferentially associated with skin allergy whereas JMADUE and Hopkins syndrome are associated with airway allergy, thus suggesting a possibility that types of preceding atopic disorders may have some influence on the sites of involvement within the spinal cord.

Among the Th2 cytokines studied, IL-4, but not IL-5 or IL-13, was found to be upregulated in JMADUE. We previously reported that in atopic myelitis both IL-4 and IL-13 production was increased while IL-5 production was not elevated [7,17], and that opticospinal multiple sclerosis at relapse showed upregulation of IL-13 but neither IL-4 nor IL-5 [8]. The present findings together with the previous ones suggest that type 2 cytokine profiles are distinct among diseases affecting the spinal cord, and that in JMADUE IL-4 may play an important role. IL-4 is a key molecule for inducing a Th2 shift and allergic inflammation through a class switch from IgM to IgE [18], as well as stimulation for eotaxin synthesis [19]. Therefore, IgE-mediated activation of mast cells and/or eosinophils triggered by IL-4 [20] may be directly involved in spinal cord damage, or alternatively IL-4 may induce anti-neuronal autoantibodies that may damage spinal motor neurons. Human platelets can be activated by IgE and are therefore involved in the IgE-mediated effector mechanisms of allergic inflammation [21]. IgE-mediated activation of platelets causes platelet aggregation and histamine release, which may induce arterial spasm, as suggested by the increased incidence of circulatory deficiencies, such as cardiovascular diseases, in atopic patients [22–25]. It is possible that such a platelet-related disturbance of the circulatory system may also occur in JMADUE, in which IgE-mediated activation as well as repeated mechanical stress could be predisposing factors for platelet aggregation [26]. Plasma exchange, previously shown to be effective in some patients with JMADUE and airway allergy, may be beneficial by removing circulating factors, such as cytokines, IgE, autoantibodies and immune complexes. Another possibility is that allergic reaction and Th2 shift may be genetically linked to JMADUE, and have no direct involvement in anterior horn cell damage. However, as there have been no pathological studies of this disease during the early progressive stages, the nature of JMADUE remains unclear.

In summary, the numbers of Th2 cells were elevated in the peripheral blood of patients with JMADUE. The Th2 cytokine and IgE-mediated immune responses may contribute to the development of spinal cord damage in this condition, although comparison with patients with atopic diseases but without JMADUE will be required in the future. Further studies on cerebrospinal fluid cytokines are also called for to clarify the involvement of immunological processes in this condition.

Acknowledgements

This work was supported in part by a Neuroimmunological Disease Research Committee grant and a Research on Brain Science grant from the Ministry of Health and Welfare, Japan, and Grants-in-Aid 12557060 and 15590894 from the Ministry of Education, Science, Sports and Culture, Japan.

References

[1] Hirayama K, Tsubaki T, Toyokura Y, Okinaka S. Juvenile muscular atrophy of unilateral upper extremity. Neurology 1963;13:373–80.
[2] Hirayama K, Tokumaru Y. Cervical dural sac and spinal cord in juvenile muscular atrophy of distal upper extremity. Neurology 2000; 54:1922–6.
[3] Hirayama K, Tomonaga M, Kitano K, Yamada T, Kojima S, Arai K. Focal cervical poliopathy causing juvenile muscular atrophy of distal

upper extremity: a pathological study. J Neurol Neurosurg Psychiatry 1987;50:285–90.
[4] Kira J, Ochi H. Juvenile muscular atrophy of the distal upper limb (Hirayama disease) associated with atopy. J Neurol Neurosurg Psychiatry 2001;70:798–801.
[5] Ochi H, Murai H, Osoegawa M, Minohara M, Inaba S, Kira J. Juvenile muscular atrophy of distal upper extremity associated with airway allergy: two cases successfully treated by plasma exchange. J Neurol Sci 2003;206:109–14.
[6] Singh VK, Mehrotra S, Agarwal SS. The paradigm of Th1 and Th2 cytokines: its relevance to autoimmunity and allergy. Immunol Res 1999;20:147–61.
[7] Ochi H, Wu XM, Osoegawa M, Horiuchi I, Minohara M, Murai H, et al. Tc1/Tc2 and Th1/h2 balance in Asian and Western types of multiple sclerosis, HTLV-1-associated myelopathy/tropical spastic paraparesis and hyperIgEaemic myelitis. J Neuroimmunol 2001; 119:297–305.
[8] Ochi H, Osoegawa M, Wu X-M, Minohara M, Horiuchi I, Murai H, et al. Increased IL-13 but not IL-5 production by CD4-positive T cells and CD8-opsitive T cells in multiple sclerosis during relapse phase. J Neurol Sci 2002;201:45–51.
[9] Schroder R, Keller E, Flacke S, Schmidt S, Pohl C, Klockgether T, et al. MRI findings in Hirayama's disease: flexion-induced cervical myelopathy or intrinsic motor neuron disease? J Neurol 1999; 246:1069–74.
[10] Willeit J, Kiechl S, Kiechl-Kohlendorfer U, Golaszewski S, Peer S, Poewe W. Juvenile asymmetric segmental spinal muscular atrophy (Hirayama's disease): three cases without evidence of "flexion myelopathy". Acta Neurol Scand 2001;104:320–2.
[11] Robberecht W, Aguirre T, Van den Bosch L, Theys P, Nees H, Cassiman JJ, et al. Familial juvenile focal amyotrophy of the upper extremity (Hirayama disease). Superoxide dismutase 1 genotype and activity. Arch Neurol 1997;54:46–50.
[12] Mizuno Y, Komori S, Shigetomo R, Kurihara E, Tamagawa K, Komiya K. Poliomyelitis-like illness after acute asthma (Hopkins' syndrome). Brain Dev 1995;17:126–9.
[13] Horiuchi I, Yamasaki K, Osoegawa M, Ohyagi Y, Okayama A, Kurokawa T, et al. Acute myelitis after asthma attacks with onset after puberty. J Neurol Neurosurg Psychiatry 2000;68:665–8.
[14] Kira J, Yamasaki K, Kawano Y, Kobayashi T. Acute myelitis associated with hyperIgEemia and atopic dermatitis. J Neurol Sci 1997;148:199–203.
[15] Kira J, Kawano Y, Yamasaki K, Tobimatsu S. Acute myelitis with hyperIgEaemia and mite antigen specific IgE: atopic myelitis. J Neurol Neurosurg Psychiatry 1998;64:676–9.
[16] Kira J, Kawano Y, Horiuchi I, Yamada T, Imayama S, Furue M, et al. Clinical, immunological and MRI features of myelitis with atopic dermatitis (atopic myelitis). J Neurol Sci 1999;162:56–61.
[17] Ochi H, Osoegawa M, Murai H, Wu X-M, Taniwaki T, Kira J. Presence of IgE antibodies to bacterial superantigens and increased IL-13-producing T cells in myelitis with atopic diathesis. Int Arch Allergy Immunol 2004;134:41–8.
[18] Gauchat JF, Lebman DA, Coffman RL, Gascan H, de Vries JE. Structure and expression of germline ε transcripts in human B cells induced by interleukin 4 to switch to IgE production. J Exp Med 1990;172:463–73.
[19] Lezcano-Meza D, Dávila-Dávila B, Vega-Miranda A, Negrete-García LM, Teran LM. Interleukin (IL)-4 and to a lesser extent either IL-13 or interferon-gamma regulate the production of eotaxin-2/CCL24 in nasal polyps. Allergy 2003;58:1011–7.
[20] Katayama I, Tanei R, Yokozeki H, Nishioka K, Dohi Y. Induction of eczematous skin reaction in experimentally anti-DNP IgE antibody: possible implications for skin lesion formation in atopic dermatitis. Int Arch Allergy Appl Immunol 1990;93:148–54.
[21] Hasegawa S, Pawankar R, Suzuki K, Nakahata T, Furukawa S, Okumura K, et al. Functional expression of the high affinity receptor for IgE (FcepsilonRI) in human platelets and its' intracellular expression in human megakaryocytes. Blood 1999;93:2543–51.
[22] Knauer KA, Lichtenstein LM, Adkinson Jr NF, Fish JE. Platelet activation during antigen-induced airway reactions in asthmatic subjects. N Engl J Med 1981;304:1404–7.
[23] Criqui MH, Lee ER, Hamburger RN, Klauber MR, Coughlin SS. IgE and cardiovascular disease. Results from a population-based study. Am J Med 1987;82:964–8.
[24] Brunekreef B, Hoek G, Fischer P, Spieksma FT. Relation between airborne pollen concentrations and daily cardiovascular and respiratory-disease mortality. Lancet 2000;355:1517–8.
[25] Ginsburg R, Bristow MR, Kantrowitz N, Baim DS, Harrison DC. Histamine provocation of clinical coronary artery spasm: implications concerning pathogenesis of variant angina pectoris. Am Heart J 1981;102:819–22.
[26] Jesty J, Yin W, Perrotta P, Bluestein D. Platelet activation in a circulating flow loop: combined effects of shear stress and exposure time. Platelets 2003;14:143–9.

ELSEVIER

Journal of the Neurological Sciences 228 (2005) 75–85

Journal of the Neurological Sciences

www.elsevier.com/locate/jns

Th1 shift in CIDP versus Th2 shift in vasculitic neuropathy in CSF

Feng-Jun Mei, Takaaki Ishizu, Hiroyuki Murai, Manabu Osoegawa, Motozumi Minohara, Kun-Nan Zhang, Jun-ichi Kira*

Department of Neurology, Neurological Institute, Graduate School of Medical Sciences, Kyushu University, 3-1-1 Maidashi, Higashi-ku, Fukuoka 812-8582, Japan

Received 17 July 2004; received in revised form 1 October 2004; accepted 6 October 2004
Available online 12 November 2004

Abstract

To investigate the intra- and extracellular levels of various cytokines and chemokines in CSF in chronic inflammatory demyelinating polyneuropathy (CIDP) and vasculitic neuropathy (VN), 16 cytokines, IL-1β, IL-2, IL-4, IL-5, IL-6, IL-7, IL-8, IL-10, IL-12 (p70), IL-13, IL-17, IFN-γ, TNF-α, G-CSF, MCP-1 and MIP-1β, were measured in CSF supernatant by a multiplexed fluorescent bead-based immunoassay and intracellular production of IFN-γ and IL-4 in CSF $CD4^+$ T cells were simultaneously measured by flow cytometry in 14 patients with CIDP, 8 patients with VN and 25 patients with other noninflammatory neurologic diseases (OND). In the CSF supernatant, a significant increase of IL-17, IL-8 and IL-6, and a significant decrease of IL-4, IL-5 and IL-7 levels were detected in pretreated CIDP as compared with OND. A significant increase of IL-6, IL-8 and IL-10 levels was found in pretreated VN. Both IL-17 and IL-8 levels correlated strongly with CSF protein levels in CIDP, although the correlation of IL-6 levels was weak. In CSF $CD4^+$ T cells, IFN-γ^+ IL-4^- cell percentages were markedly elevated in CIDP compared with OND, but not in VN, resulting in a significant increase of intracellular IFN-γ/IL-4 ratio in CIDP, even in the absence of CSF pleocytosis. The nonresponders to intravenous immunoglobulins (IVIGs) showed a significantly lower IFN-γ^- IL-4^+ $CD4^+$ T cell percentage, and tended to have a higher intracellular IFN-γ/IL-4 ratio than the responders in CSF. Marked upregulation of Th1 cytokine, IL-17, and downregulation of Th2 cytokines, together with infiltration of IFN-γ-producing $CD4^+$ T cells are useful markers for CIDP, while several Th2 cytokines are upregulated in VN in CSF.

Keywords: Th1; Th2; CSF; Cytokine; CIDP; Vasculitic neuropathy

1. Introduction

Chronic inflammatory demyelinating polyneuropathy (CIDP) is regarded as an autoimmune disease targeting peripheral nerve myelin, although its mechanism remains unknown. Immunohistochemical studies of biopsied sural nerves revealed that both $CD4^+$ and $CD8^+$ T cells infiltrated together along with activated macrophages but without either B cells or immunoglobulin deposition [1,2], suggesting a critical role for T cells. On the other hand, humoral immunity, such as immunoglobulins and immune complexes, is believed to be involved in vasculitic neuropathy (VN) [3].

Chemokines are crucial for recruiting T cells to inflammatory sites. Recent studies on chemokines in CIDP CSF revealed an increase in chemokines, attracting mainly Th1 cells, such as CXCL10 (IP-10) [4,5], which coincides with the highest expression of CXCR3. CXCR3 is a chemokine receptor for CXCL10 and is specific for Th1 cells among chemokine receptors in the invading T cells in biopsied sural nerves [4]. However, the significance of the increase in chemokines in CSF still remains unclear, as there is no CSF pleocytosis in CIDP, and none of the studies found any changes in the cellular composition of CSF in this condition.

Moreover, in CIDP CSF, cytokines such as IL-1α, IL-1β, IL-2, IL-6, IL-10, IFN-γ, TNF-α and monocyte colony-stimulating factor (M-CSF) were all found to be negative by an enzyme-linked immunosorbent assay (ELISA) [6], except for in one earlier study that showed an increase of

* Corresponding author. Tel.: +81 92 642 5340; fax: +81 92 642 5352.
E-mail address: kira@neuro.med.kyushu-u.ac.jp (J. Kira).

0022-510X/$ - see front matter © 2004 Elsevier B.V. All rights reserved.
doi:10.1016/j.jns.2004.10.001

IL-6 [7]. However, a fluorescent bead-based immunoassay, with a wide dynamic range of standard curves, for multiple cytokines has become available, and requires only small amounts of materials for simultaneous measurements of multiple cytokines [8,9]. Therefore, the present study aimed to directly measure the intracellular cytokine production of $CD4^+$ T cells by flow cytometry, and various cytokine and chemokine levels of the CSF supernatant by multiplexed fluorescent bead-based immunoassay in CIDP and vasculitic neuropathy (VN). This was done to clarify the distinct immune balance in the CSF compartment. In addition, since CSF is considered to reflect events within the blood nerve barrier (BNB) more than in peripheral blood, we wanted to determine clinically useful CSF markers for each inflammatory neuropathy.

2. Materials and methods

2.1. Subjects

Fourteen patients with probable CIDP (9 males and 5 females, mean age±S.D.=60.1±17.2 years, range 28–80) based on the criteria of the American Academy of Neurology AIDS Task Force, were enrolled in this study [10]. In addition, 8 patients with untreated VN presented as mononeuritis multiplex (4 males and 4 females, mean age±S.D.=48.1±16.1 years, range 19–66) and 25 patients with other noninflammatory neurologic diseases (OND; 14 males and 11 females, mean age±S.D.=56.5±14.7 years, range 20–80) were also enrolled in the study. The OND group was composed of 14 patients with spinocerebellar degeneration, 2 with amyotrophic lateral sclerosis, 2 with cervical spondylosis, 2 with Alzheimer's disease and 1 each with Parkinson's disease, progressive supranuclear palsy, myelopathy, spinal cord infarction and epilepsy. The duration of CIDP ranged from 2 months to 24 years (mean±S.D.=6.69±8.95 years) at the time of lumbar puncture. Clinical courses were chronic progressive in 7, relapsing–remitting in 6 and monophasic in 1. Hughes grades [11] were 2 to 4 (mean±S.D.=3.21±0.89). All patients with CIDP showed motor dominant involvement and all but three showed symmetrical involvement. Eleven patients were treated by intravenous immunoglobulin (IVIG; 0.4g/kg/day) infusion for 5 days, and the six who improved by one or more than one grade on the Hughes scale after therapy were considered to be responders (Table 1).

2.2. Sample collection

At least 5 ml each of CSF and blood samples were obtained from all patients. In the case of CIDP, 26 CSF samples from 14 patients, 19 pretreatment and 7 posttreatment were obtained; all 8 CSF samples from the 8 VN patients were those from pretreatment. CSF samples were immediately centrifuged at 800 rpm/min at 4 °C for 5 min. The CSF cell counts in the samples used for the intracellular cytokine analysis were 2.0±1.0/μl (mean±S.D., range 1.0–4.0) in CIDP patients, 5.0±4.0/μl (mean±S.D., range 1.0–12.0) in VN patients and 1.0±0.5/μl (mean±S.D., range 1.0–2.0) in OND patients. CSF supernatant was kept under −70 °C until the cytokine assay.

2.3. Multiplexed fluorescent bead-based immunoassay

CSF supernatants were collected and analyzed simultaneously for 16 different cytokines and chemokines, namely, IL-1β, IL-2, IL-4, IL-5, IL-6, IL-7, IL-8, IL-10, IL-12 (p70), IL-13, IL-17, IFN-γ, TNF-α, granulocyte colony-stimulating factor (G-CSF), monocyte chemoattractant protein 1 (MCP-1) and macrophage inflammatory protein 1β (MIP-

Table 1
Demographic features of patients with CIDP

Patient no.	Age at onset (year)	Age at examination (year)	Sex	Duration	Hughes grade at peak	CSF cells/protein (/μl, mg/dl)	Clinical course	Response to IVIG	Clinical symptoms	
									Predominant symptoms	Symmetrical involvement
1	58	65	M	7 y	2	2/148	relapsing	good	motor>sensory	+
2	72	72	F	2 m	2	1/28	monophasic	good	motor>sensory	−
3	27	28	M	1 y	4	2/87	relapsing	good	motor>>sensory	+
4	58	59	F	4 m	2	4/69	relapsing	good	motor>>sensory	+
5	75	77	F	3 y	4	1/253	CP	good	motor>sensory	+
6	49	53	M	4 y	4	1/39	CP	good	motor>>sensory	+
7	79	80	M	1 y	4	2/36	CP	poor	motor>>sensory	+
8	75	76	F	1 y	4	4/45	CP	poor	motor>>sensory	−
9	40	64	M	24 y	4	2/102	CP	poor	motor>sensory	+
10	60	80	M	20 y	4	2/68	relapsing	poor	motor>sensory	+
11	37	39	M	2 y	2	1/72	CP	poor	motor>sensory	+
12	12	36	M	24 y	3	1/30	relapsing	NE	motor	+
13	46	46	M	2 m	3	1/127	CP	NE	motor>sensory	+
14	61	67	F	6 y	3	0/30	relapsing	NE	motor	−

CIDP: chronic inflammatory demyelinating polyneuropathy, M: male, F: female, m: months, y: years, CSF: cerebrospinal fluid, IVIG: intravenous immunoglobulin, CP: chronic progressive, NE: not examined.

1β) using the Bio-Plex Cytokine Assay System (Bio-Rad Laboratories, Hercules, CA) according to the manufacturer's instructions [8,9]. Briefly, 50 μl of each CSF supernatant and various concentrations of each cytokine standard (Bio-Rad) were added to 50 μl of antibody-conjugated beads (Bio-Rad) in a 96-well filter plate (Millipore, Billerica, MA). After a 30-min incubation, the plate was washed and 25 μl of a biotinylated antibody solution (Bio-Rad) was added to each well, followed by another 30-min incubation. The plate was then washed and 50 μl of streptavidin-conjugated PE (Bio-Rad) was added to each well and incubated for 10 min. Following a final wash, the contents of each well were resuspended in 125 μl of the assay buffer (Bio-Rad) and analyzed using a Bio-Plex Array Reader (Bio-Rad). The cytokine concentrations were calculated by reference to a standard curve for each cytokine derived using various concentrations of the cytokine standards (0.2, 0.78, 3.13, 12.5, 50, 200, 800 and 3200 pg/ml) assayed in the same manner as the CSF samples. The detection limit of each cytokine was determined by the recovery of the corresponding cytokine standard, and the lowest values showing more than 50% recovery were set as the lower detection limits. The lower detection limit for each cytokine was as follows: 0.2 pg/ml for IL-2, IL-4, IL-5, IL-7, IL-8, IL-10, IL-12 (p 70), IL-13, IL-17, IFN-γ and TNF-α, 0.78 pg/ml for IL-1β and IL-6, and 3.13 pg/ml for G-CSF, MCP-1 and MIP-1β. All samples were analyzed undiluted in duplicate. CSF supernatants used for the multiplexed fluorescent bead-based immunoassay were 26 CIDP (19 pre- and 7 posttreatment), 8 VN and 24 OND samples.

2.4. Intracellular cytokine analysis by flowcytometry

Each CSF supernatant was carefully removed and cell sediments were suspended in RPMI 1640 (Nipro, Tokyo, Japan) supplemented with 10% fetal calf serum (FCS; Gibco BRL, Gaithersburg, MD; Lot#3217341S). This was followed by incubation with 25 ng/ml of phorbol 12-myristate 13-acetate (PMA; Sigma, St. Louis, MO), 1.0 μg/ml of ionomycin (Sigma) and 10 μg/ml of Brefeldin A (BFA; Sigma) in a 24-well plate at 37 °C for 4 h under 5% CO_2. After washing with phosphate-buffered saline containing 0.1% bovine serum albumin (0.1% BSA-PBS), cells were stained with perCP-conjugated anti-CD4 monoclonal antibodies (Immunotech, Marseille, France) and incubated on ice in the dark for 15 min. Following another wash with 0.1% BSA-PBS, FACS permeabilizing solution (Becton Dickinson, San Jose, CA) was added and the cells were placed in the dark for 10 min. After two washes with 0.1% BSA-PBS, the cells were then stained with FITC-conjugated anti-IFN-γ (Immunotech) and PE-conjugated anti-IL-4 (Immunotech) for intracellular cytokine analysis, with mouse IgG2a-FITC (Immunotech) and IgG1-PE (Immunotech) as controls. After a 30-min incubation on ice in the dark, the percentages of intracellular IFN-γ-and IL-4-producing cells were immediately analyzed flowcytometrically using an Epics XL System II (Coulter, Hialeah, FL). Analysis gates were first set on lymphocytes according to the forward and side scatter properties and then set on $CD4^+$ lymphocytes. Cases with $CD4^+$ cell counts of less than 500 were discarded from the analysis to increase the reliability. For peripheral blood lymphocytes (PBL), intracellular cytokines were studied as described previously [12], using the same amounts of PMA, ionomycin and BFA, and the same monoclonal antibodies for staining. CSF cells taken from 10 patients with pretreated CIDP, 8 with VN at the pretreatment time and 12 OND patients, were used for intracellular cytokine analysis.

2.5. Statistical analysis

Statistical analyses were performed by the nonparametric Mann–Whitney U test to determine the significance between OND and each disease group. The difference between CSF and PBL in each group was analyzed by Wilcoxon signed rank test. In the CIDP group, the difference between responders and nonresponders was also analyzed by Mann–Whitney U test.

3. Results

3.1. Detection rates of each cytokine in CSF supernatant

The detection rate of IL-17 was significantly higher in pretreated CIDP patients compared with OND patients (19/19, 100% vs. 11/24, 45.8%, p=0.0004) and that of IL-10 was also significantly higher in VN patients (8/8, 100% vs. 11/24, 45.8%, p=0.0104), while that of IL-4 was significantly lower in pretreated and posttreated CIDP patients (10/19, 52.6% vs. 23/24, 95.8%, p=0.0022 and 3/7, 42.9% vs. 23/24, 95.8%, p=0.0051, respectively; Fig. 1). The detection rates of other cytokines were not significantly different between OND patients and each disease condition. IL-2 and IL-12 (p70) were not used for further statistical analyses because of low detection rates in CSF.

3.2. Comparison of cytokine levels in CSF supernatant among diseases

In CIDP patients, IL-17, IL-8 and IL-6 levels were significantly increased at the time of pretreatment as compared with OND levels (10.32±7.69 vs. 4.39±6.02 for the mean±S.D. and 10.33 vs. 0.19 for the median, p=0.0019; 31.17±19.99 vs. 14.23±9.20 and 25.50 vs. 11.32, p=0.0020; 42.94±27.82 vs. 62.89±179.80 and 30.29 vs. 21.55, p=0.0060, respectively; Fig. 2). After IVIG, the increase of IL-8 levels was still significant (31.62±12.26 vs. 14.23±9.29 and 32.00 vs. 11.32, p=0.0025) but not those of IL-17 (9.59±6.50 vs. 4.39±6.02 and 9.22 vs. 0.19) and IL-6 (44.94±26.26 vs. 62.89±179.77 and 31.95 vs. 21.55). In contrast, IL-4, IL-5

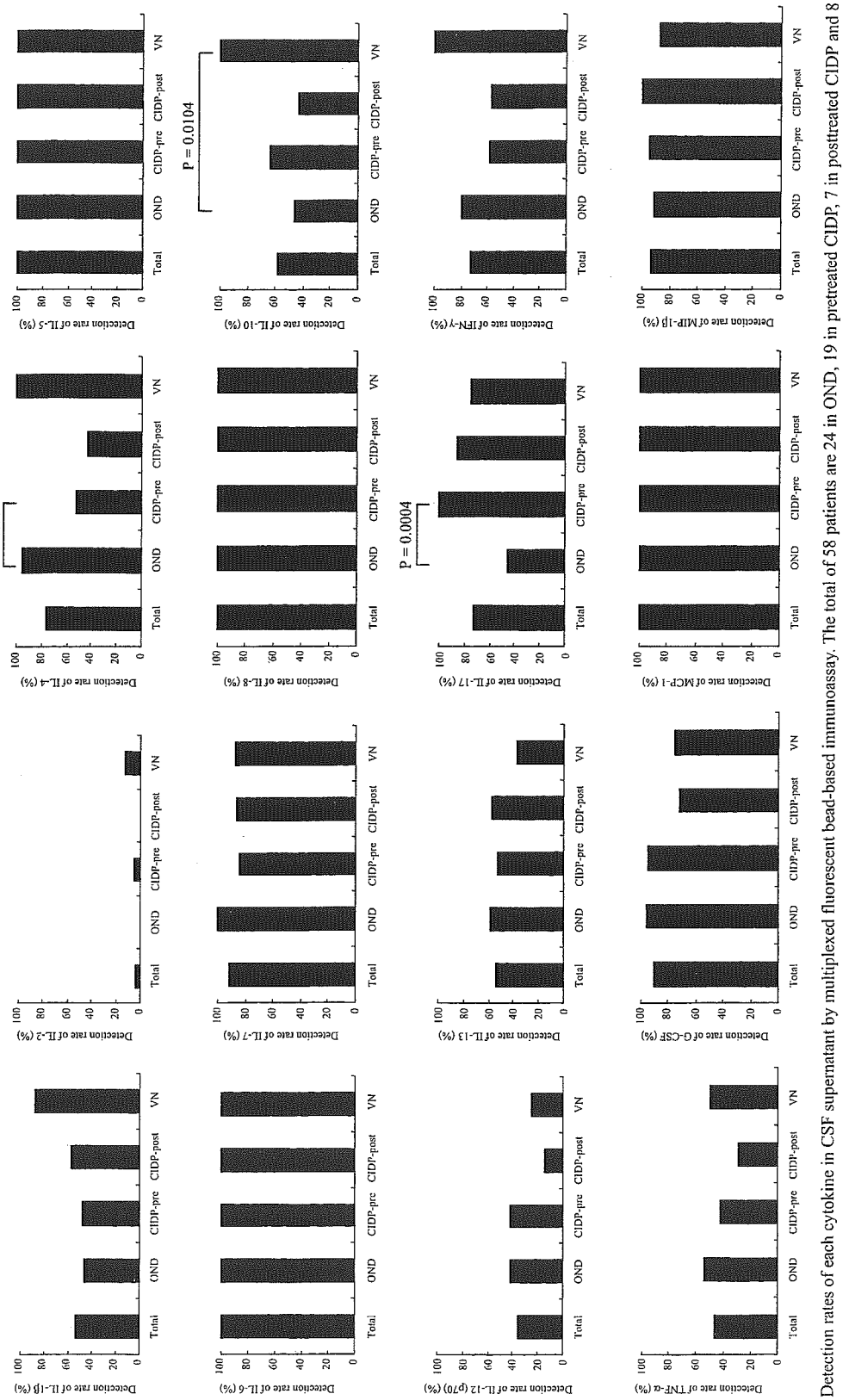

Fig. 1. Detection rates of each cytokine in CSF supernatant by multiplexed fluorescent bead-based immunoassay. The total of 58 patients are 24 in OND, 19 in pretreated CIDP, 7 in posttreated CIDP and 8 in VN.

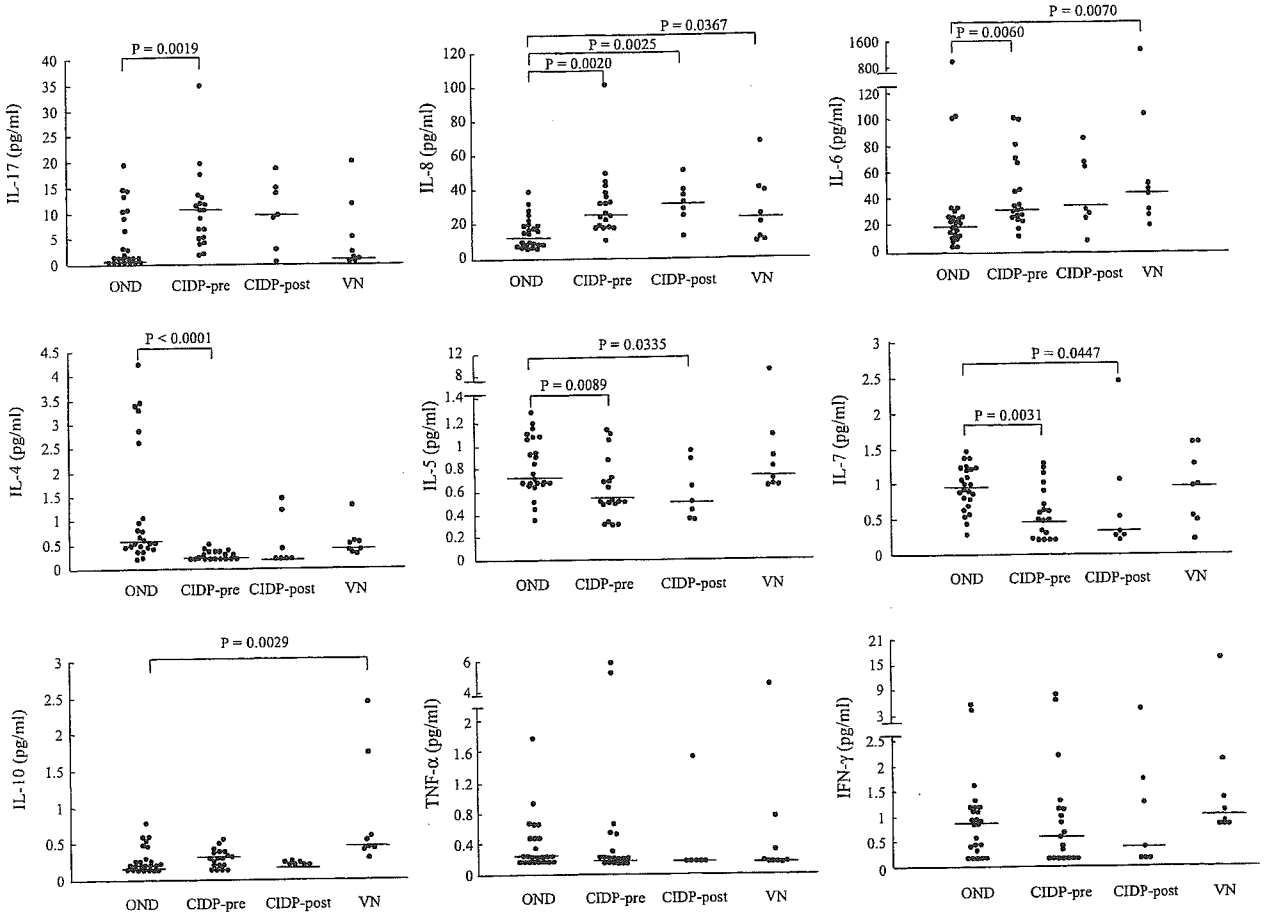

Fig. 2. Cytokine levels in the CSF supernatant in OND, CIDP and VN by multiplexed fluorescent bead-based immunoassay. CIDP-pre=CIDP at the pretreatment. CIDP-post=CIDP after the IVIG (6 patients were responders and 5 nonresponders). IL-1β, IL-13, G-CSF, MCP-1 and MIP-1β are not shown in the figure, but mean±S.D. and median values of these cytokines are given in the text. IL-2 and IL-12 (p70) are not shown due to the low detection frequency in CSF.

and IL-7 levels were significantly decreased at pretreatment (0.27±0.09 vs. 1.22±1.26 and 0.22 vs. 0.55, $p<0.0001$, 0.62±0.26 vs. 0.82±0.25 and 0.57 vs. 0.74, $p=0.0089$, and 0.58±0.36 vs. 0.94±0.31 and 0.48 vs. 0.95, $p=0.0031$, respectively). At the time of posttreatment, decreases of IL-5 and IL-7 levels were still significant (0.59±0.24 vs. 0.82±0.25 and 0.52 vs. 0.74, $p=0.0335$, and 0.72±0.81 vs. 0.94±0.31 and 0.31 vs. 0.95, $p=0.0447$, respectively) but this was not the case for IL-4 levels (0.54±0.53 vs. 1.22±1.26 and 0.19 vs. 0.55). None of the other cytokines or chemokines showed any significant changes at either the pre- or posttreatment times. The concentrations of the other cytokines and chemokines, which did not show any significant changes, were as follows in the pretreatment CIDP, posttreatment CIDP and OND patients: IL-1β (pg/ml), 1.55±1.11 (mean±S.D.) and 0.77 (median), 2.25±2.56 and 0.93, and 1.36±0.73 and 0.77; IL-13 (pg/ml), 0.77±1.05 and 0.20, 0.9±1.55 and 0.34, and 0.65±0.76 and 0.24; IFN-γ (pg/ml), 1.47±2.55 and 0.53, 1.16±1.47 and 0.43, and 1.05±1.18 and 0.81; G-CSF (pg/ml), 33.24±29.61 and 21.11, 14.74±9.70 and 18.20, and 25.35±21.50 and 19.85; MCP-1 (pg/ml), 219.05±154.72 and 169.71, 145.97±89.18 and 99.55, and 174.3±69.31 and 160.32; MIP-1β (pg/ml), 11.05±6.3 and 10.80, 13.31±7.9 and 12.79, and 16±13.85 and 10.28; IL-10, (pg/ml) 0.29±0.11 and 0.29, 0.21±0.02 and 0.19, and 0.30±0.17 and 0.19; TNF-α (pg/ml) 0.80±1.64 and 0.19, 0.42±0.46 and 0.19, and 0.36±0.32 and 0.20, respectively.

In contrast, VN patients showed a significant increase of IL-6, IL-8 and IL-10 levels as compared with OND patients at the time of pretreatment (208.54±457.09 vs. 62.89±179.77 and 43.41 vs. 21.55, $p=0.0070$, 27.52±20.30 vs. 14.23±9.29 and 22.53 vs. 11.32, $p=0.0367$, and 0.85±0.78 vs. 0.30±0.17 and 0.48 vs. 0.19, $p=0.0029$, respectively). There were no significant changes in concentration of any of the other cytokines and chemokines in VN patients, and the results are as follows: IL-1β (pg/ml), 1.63±1.52 (mean±S.D.) and 1.16 (median); IL-4 (pg/ml), 0.53±0.33 and 0.44; IL-5 (pg/ml), 1.80±2.91 and 0.75; IL-7 (pg/ml), 0.94±0.52 and 0.95; IL-13 (pg/ml), 0.64±0.75 and 0.19; IL-17 (pg/ml), 5.07±7.07 and 1.58; IFN-γ (pg/ml), 2.98±5.45 and 1.0; TNF-α (pg/ml), 0.77±1.41 and 0.20; G-CSF (pg/ml), 30.52±22.55 and 35.02; MCP-1 (pg/ml), 182.22±96.40 and 169.82; MIP-1β (pg/ml), 9.47±5.04 and 6.67.

3.3. Comparison of intracellular cytokine production between CSF cells and PBL

Representative staining patterns for the cytokines in each group are shown in Fig. 3. CSF cells showed a significantly higher proportion of IFN-γ^+ IL-4$^-$ CD4$^+$ T cells than in PBL in CIDP patients (p=0.0051), VN (p=0.0117) and OND patients (p=0.0022; Fig. 4). IFN-γ^- IL-4$^+$ CD4$^+$ T cell percentages were significantly lower in CSF cells than in PBL in VN patients (p=0.0421) and OND patients (p=0.0342), and also tended to be lower in CIDP patients (p=0.0745). Thus, the intracellular IFN-γ/IL-4 ratio (IFN-γ^+ IL-4$^-$ CD4$^+$ T cell percentage divided by IFN-γ^- IL-4$^+$ CD4$^+$ T cell percentage) was significantly higher in CSF cells than in PBL in CIDP patients (p=0.0051), VN (p=0.0117) and OND patients (p=0.0029). IFN-γ^+ IL-4$^+$ cell percentages were significantly greater in CSF cells than in PBL in CIDP patients (p=0.0284), VN (p=0.0117) and OND patients (p=0.0229).

3.4. Comparison of intracellular cytokine production of CSF cells and PBL among diseases

In CSF cells, IFN-γ^+ IL-4$^-$ cell percentages in CIDP patients showed clustering in the high ranges, while those in VN patients were distributed over a wide range (Fig. 4). Thus, IFN-γ^+ IL-4$^-$ cell percentages were markedly increased in CIDP compared with OND patients (p=0.0008), but not in

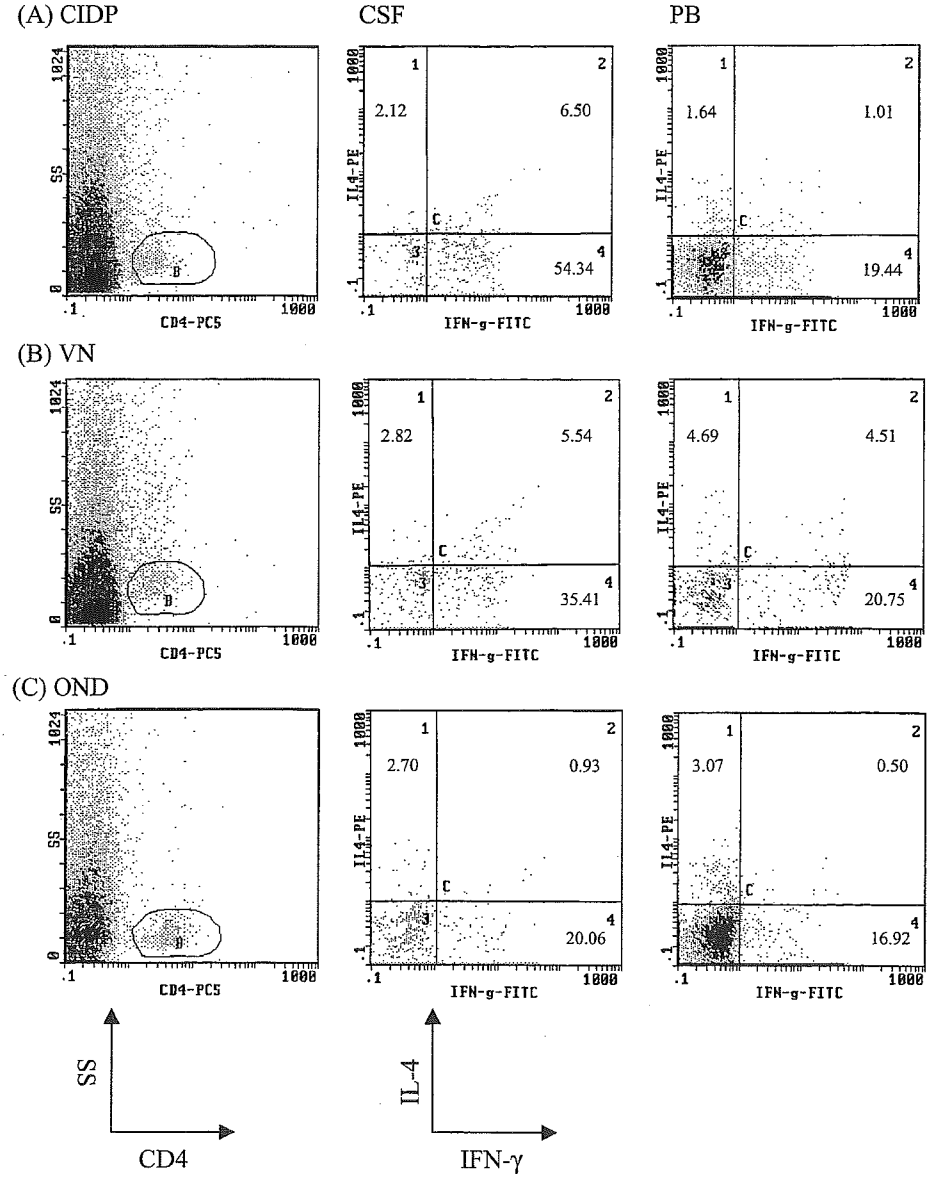

Fig. 3. Representative staining patterns of the intracellular cytokines in CSF CD4$^+$ T cells and peripheral blood (PB) CD4$^+$ T cells from CIDP, VN and OND patients. (A) A 59-year-old patient with CIDP. (B) A 51-year-old patient with VN. (C) A 52-year-old patient with amyotrophic lateral sclerosis. Note the increase in IFN-γ^+ IL-4$^-$ CD4$^+$ T cells in the CIDP CSF cells compared with OND.

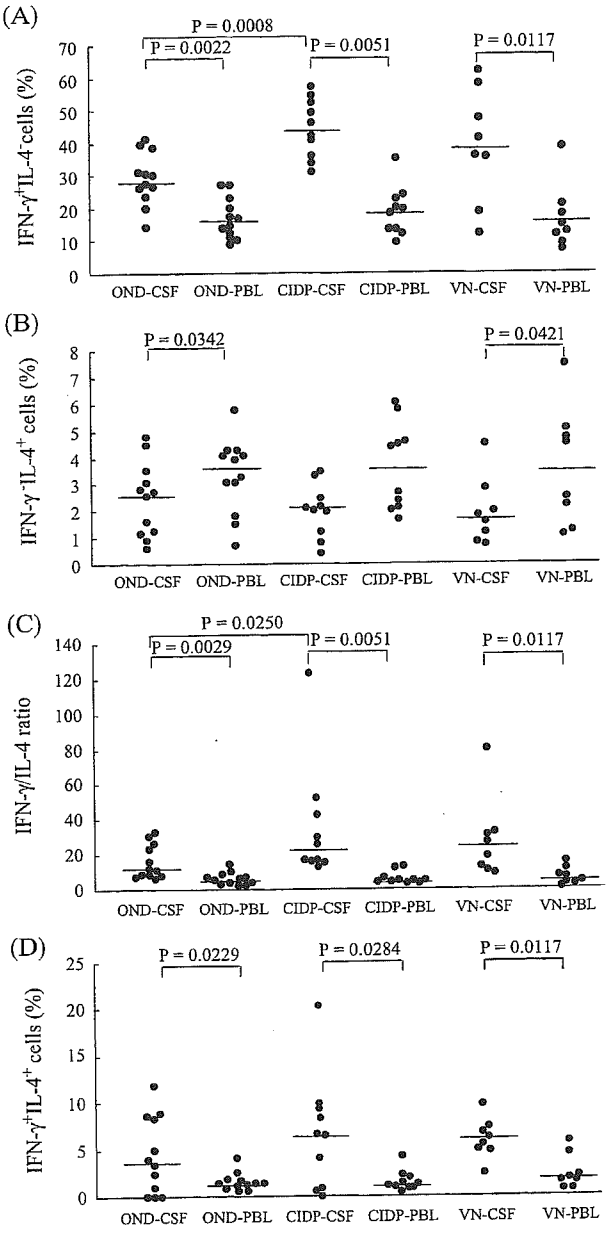

Fig. 4. Intracellular cytokine production patterns of CSF $CD4^+$ T cells in CIDP, VN and OND. (A) IFN-γ^+ IL-4^- $CD4^+$ T cell percentages. (B) IFN-γ^- IL-4^+ $CD4^+$ T cell percentages. (C) Intracellular IFN-γ/IL-4 ratios in $CD4^+$ T cells. (D) IFN-γ^+ IL-4^+ $CD4^+$ T cell percentages.

VN patients, while in PBL, the percentages did not differ significantly among the diseases. IFN-γ^- IL-4^+ cell percentages were not significantly different among the groups in either CSF cells or PBL. Thus, the intracellular IFN-γ/IL-4 ratio was significantly increased in CSF cells in CIDP compared with OND patients (p=0.0250). The ratios in CSF in VN patients, and in PBL in either CIDP or VN patients were not significantly different compared with OND patients. The proportions of IFN-γ^+ IL-4^+ cells in either CSF cells or PBL were not significantly different among the groups.

3.5. Correlation between clinical parameters and intra- and extracellular cytokine levels in CIDP patients

Both IL-17 and IL-8 in CSF supernatant showed significant positive correlation with CSF protein concentrations (r=0.468, p=0.0027 and r=0.579, p=0.0022, respectively; Fig. 5). CIDP patients with increased CSF protein levels at examination had significantly higher levels

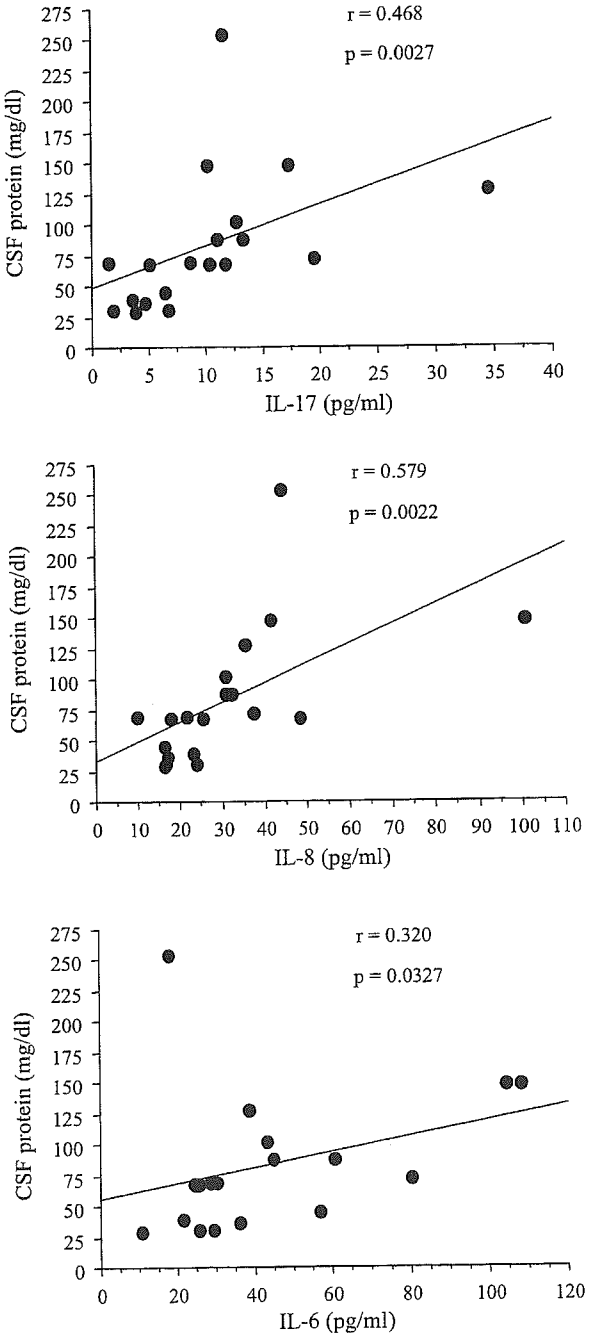

Fig. 5. Correlation between IL-17, IL-8 and IL-6 levels in CSF supernatant and CSF protein concentration. Both IL-17 and IL-8 in CSF supernatant showed a strong positive correlation with CSF protein concentration, while IL-6 showed a weak correlation with CSF protein levels.

of IL-17 and IL-8 than those without the protein increase (12.5±7.83 vs. 4.21±1.75 for the mean±S.D. and 11.39 vs. 3.94 for the median, p=0.0095 in IL-17, and 35.31±21.88 vs. 19.57±3.79 and 31.88 vs. 17.33, p=0.0464 in IL-8). IL-6 levels also showed a weak correlation with CSF protein levels (r=0.320, p=0.0327), and IL-6 levels in CSF tended to be higher in CIDP patients with increased CSF protein levels than in those without the increase (49.4±29.54 vs. 24.83±9.52 and 41.16 vs. 25.85, p=0.0641). In CSF cells of CIDP patients, IVIG nonresponders showed significantly lower IFN-γ^- IL-4^+ $CD4^+$ T cell percentages in CSF at pretreatment than responders (p=0.0105), and the intracellular IFN-γ/IL-4 ratio also tended to be higher in nonresponders than responders (p=0.0811; Fig. 6). No other clinical parameters, such as age at onset or at examination, duration of disease, sex, clinical course and Hughes grade, had any significant correlation with intra- and extracellular cytokine amounts in CSF.

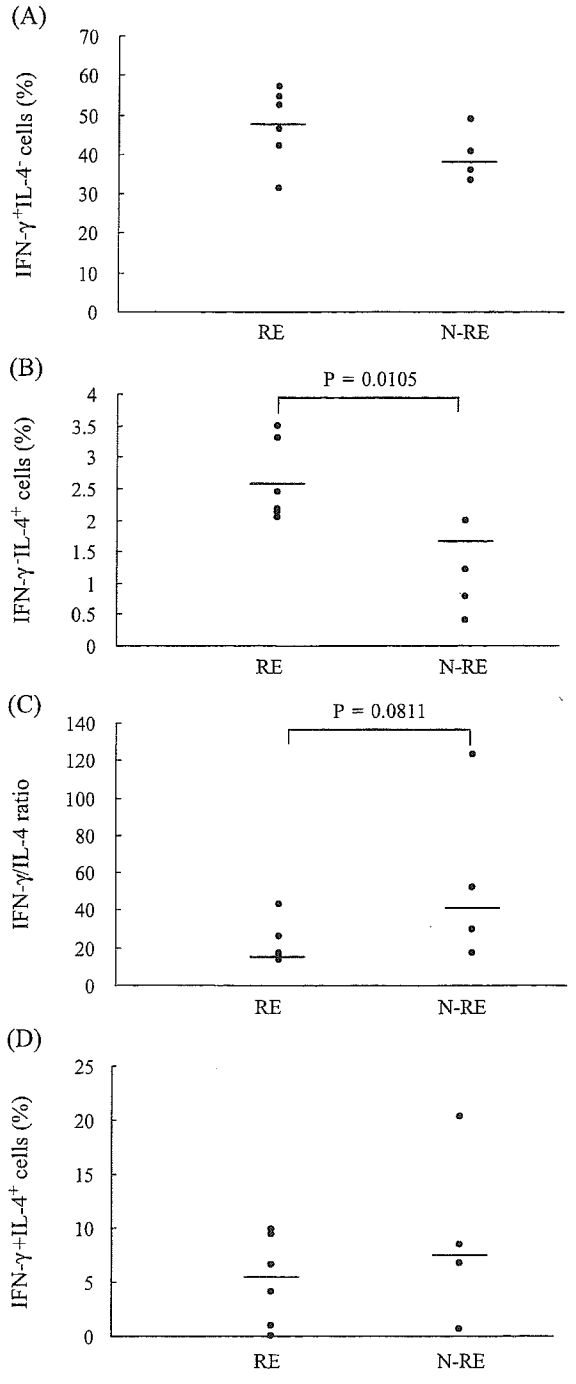

Fig. 6. Comparison of intracellular cytokine production patterns between IVIG responders (RE) and nonresponders (N-RE) in CIDP. (A) IFN-γ^+ IL-4^- $CD4^-$ T cell percentages. (B) IFN-γ^-IL-4^- $CD4^+$ T cell percentages. (C) Intracellular IFN-γ/IL-4 ratios in $CD4^+$ T cells. (D) IFN-γ^+ IL-4^+ $CD4^+$ T cell percentages.

4. Discussion

The present study is the first to demonstrate changes in intracellular cytokine production in CSF cells and changes in secreted cytokine levels in CSF supernatant, by a combined intra- and extracellular cytokine analysis in CIDP and VN. Our method successfully measured the intracellular cytokine production even in the absence of CSF pleocytosis. Cytokine assessment at the cellular level in the CSF has been difficult because of the extreme fragility of CSF cells and their limited numbers. In the current study, even in the absence of CSF pleocytosis, CIDP patients were found to have a marked increase in IFN-γ-producing $CD4^+$ T cells and thus a greater Th1 shift in the CSF compartment than OND patients, which coincided with upregulation of type 1 cytokine, IL-17, and downregulation of type 2 cytokines, such as IL-4 and IL-5. In contrast, VN patients showed upregulation of type 2 cytokines, such as IL-6 and IL-10.

Among the cytokines that were elevated in the CSF supernatant in the pretreated patients, IL-17 was upregulated in CIDP patients but not in VN patients. In addition, IL-10 was elevated in VN patients but not in CIDP patients, whereas both IL-6 and IL-8 levels were upregulated in CIDP patients as well as VN patients, suggesting unique roles for IL-17 in CIDP and IL-10 in VN. IL-17 is a potent proinflammatory cytokine produced by a subset of memory $CD4^+$ T cells, mainly Th1 type, on activation [13–15]. IL-17 triggers the local production of downstream cytokines and chemokines, such as IL-6, IL-8, MCP-1 and G-CSF, from a wide variety of cells [13,15,16]. It is possible that increase of IL-6 and IL-8 found in the present study may be triggered by IL-17. In addition, IL-17 stimulates the production of matrix metalloproteinases [17,18], iNOS, NO [19,20] and PGE2 [13,21], which enhance the local inflammatory environment; as shown in rheumatoid arthritis (RA) where high levels of IL-17 in synovial fluid contribute to inflammatory joint destruction [22,23]. In the present study, both IL-17 and IL-8 levels positively correlated with CSF protein concentrations in CIDP patients, which indicates that an increase of those cytokines/chemokines is related to the severity of inflammation in the spinal roots. Both IL-6 and IL-8 are proinflammatory cytokines and contribute to exacerbate various

autoimmune inflammatory diseases, such as rheumatoid arthritis (RA) [24], systemic lupus erythematosus (SLE) [25], ulcerative colitis [26], Crohn's disease [27] and psoriasis [24]. IL-6 induces an acute phase response, activates monocytes [28] and induces other chemokines [29], such as MIP-2, and adhesion molecules [30]; while IL-8 recruits granulocytes and T cells to the local inflammatory sites [31,32]. Therefore, increased IL-6 and IL-8 responses could also contribute to enhance local inflammation in CIDP.

In contrast, type 2 cytokines, IL-4 and IL-5, were downregulated in CSF supernatant only in CIDP patients. IL-7, which was originally described as a growth and differentiation factor for precursor B cells [33] and was later shown to prime human naïve $CD4^+$ T cells for IFN-γ as well as IL-4 [34], was downregulated in CIDP CSF in the present study. The underlying disease process of CIDP appears to cause this cytokine to behave similarly to type 2 cytokines. This finding is similar to those in other organ-specific autoimmune diseases, such as bullous pemphigoid, where IL-7 is downregulated more in the blister fluid than in the sera [35].

IVIG treatment has been shown to be effective in CIDP and can shift the immune balance from the Th1 to the Th2 side [36,37]. Therefore, the beneficial effects of giving IVIG in CIDP are at least partly attributable to the correction of the pathogenic Th1 shift. However, since the nonresponders to IVIG showed significantly lower IFN-γ^- IL-4^+ $CD4^+$ T cells than responders, IVIG does not appear able to overcome the disease process in CIDP patients with markedly depressed Th2 cells in CSF.

Mathey et al. [38] showed that mRNA expression of Th1 cytokines, such as IFN-γ, TNF-α and IL-2, was upregulated in the biopsied sural nerves from CIDP patients. However, in CSF supernatant, IL-2 was barely detectable in any of the diseases examined, and the increases of TNF-α and IFN-γ concentrations were not statistically significant. Although one ELISA study has demonstrated an increase of TNF-α concentrations in CIDP sera in a fraction of patients with grave disability [39], in the present study, only a minority of CIDP patients with grave disease (Hughes grade 4) had very high TNF-α concentrations in CSF. This observation might be explained by the very short half life of TNF-α, i.e., 30 min [40], or alternatively, a distinct subset of CIDP patients may preferentially produce TNF-α. For IFN-γ, intracellular cytokine analysis is superior to extracellular cytokine measurement; probably because intracellular cytokine analysis measures the preprogrammed potential of cytokine production in each cell directly, and thus the amounts are not diluted by other factors, such as large volumes of continually replacing CSF.

Although we previously reported that Th2 cells are also increased in peripheral blood in some CIDP patients by intracellular cytokine analysis [41], Th1 shift is evident in CSF cells. It is possible that Th1 cells move from peripheral blood to nerves beyond the BNB, and CSF cells more sensitively reflect the pathological process occurring within the BNB in CIDP.

In the present study, IL-6, IL-8 and IL-10 levels were found to be upregulated in CSF supernatant in VN patients; a group in which CSF cytokine changes have never been reported. In addition, acting as a proinflammatory cytokine, IL-6 increases fibrinogen amounts [42] and platelet number [43], and increases blood viscosity through the induction of hepatic acute phase response [24]. Therefore, it is possible that an increase of IL-6 exacerbates vasculitis-related ischemia of the peripheral nerves. Furthermore, both IL-6 and IL-10 can enhance autoantibody production [24,25,44–46]. Although the increase of IL-10 in VN could be the result of the host's efforts to counteract inflammation since IL-10 works as anti-inflammatory cytokine [47], IL-10 itself is regarded as an exacerbating factor in vasculitic disorders, such as SLE [25,48], RA [46], Sjögren's syndrome [44] and Wegener's granulomatosis [45], through enhanced autoantibody production. As immunoglobulins, complements and immune complexes are deposited in the vessel wall in VN [3,49], enhanced IL-6 and IL-10 responses in CSF may act as exacerbating factors in this condition.

Since no increase of intracellular IFN-γ/IL-4 ratio in CSF cells was observed in VN patients, the commitment of Th1 cells may be less important in VN than in CIDP. However, intracellular IFN-γ^+ IL-4^- $CD4^+$ cell percentages in VN CSF were distributed over a wide range, which is in contrast to the clustering observed in the high ranges in CIDP patients. This indicates the heterogeneous nature of VN and further investigation of CSF intracellular cytokine analyses together with further subclassification of VN is required.

In conclusion, our combined multiplexed fluorescent bead-based immunoassay and intracellular cytokine analysis of CSF successfully demonstrated the upregulation of Th1 and downregulation of Th2 cytokines, increased IFN-γ producing $CD4^+$ T cells in CIDP patients and the upregulation of some Th2 cytokines in VN patients. Thus, we propose that IL-4, IL-5, IL-6, IL-7, IL-8, IL-10 and IL-17 are clinically useful sets of cytokines for CSF immune monitoring by multiplexed fluorescent bead-based immunoassay.

Acknowledgements

This work was supported in part by a Neuroimmunological Disease Research Committee grant, a Research on Brain Science grant from the Ministry of Health and Welfare, Japan, and Grants 12470142, 12557060 and 12877097 from the Ministry of Education, Science, Sports and Culture, Japan.

References

[1] Matsumuro K, Izumo S, Umehara F, Osame M. Chronic inflammatory demyelinating polyneuropathy: histological and immunopathological studies on biopsied sural nerves. J Neurol Sci 1994;127:170–8.
[2] Rizzuto N, Morbin M, Cavallaro T, Ferrari S, Fallahi M, Galiazzo Rizzuto S. Focal lesions area feature of chronic inflammatory

demyelinating polyneuropathy (CIDP). Acta Neuropathol (Berl) 1998; 96:603–9.
[3] Davies L, Spies JM, Pollard JD, McLeod JG. Vasculitis confined to peripheral nerves. Brain 1996;119:1441–8.
[4] Kieseier BC, Tani M, Mahad D, Oka N, Ho T, Woodroofe N, et al. Chemokines and chemokine receptors in inflammatory demyelinating neuropathies: a central role for IP-10. Brain 2002;125:823–34.
[5] Mahad DJ, Howell SJL, Woodroofe MN. Expression of chemokines in cerebrospinal fluid and serum of patients with chronic inflammatory demyelinating polyneuropathy. J Neurol Neurosurg Psychiatry 2002; 73:320–3.
[6] Sivieri S, Ferrarini AM, Lolli F, Matà S, Pinto F, Tavolato B, et al. Cytokine pattern in the cerebrospinal fluid from patients with GBS and CIDP. J Neurol Sci 1997;147:93–5.
[7] Maimone D, Annunziata P, Simone IL, Livrea P, Guazzi GC. Interleukin-6 levels in the cerebrospinal fluid and serum of patients with Guillain–Barré syndrome and chronic inflammatory demyelinating polyradiculoneuropathy. J Neuroimmunol 1993;47:55–61.
[8] Vignali DAA. Multiplexed particle-based flow cytometric assays. J Immunol Methods 2000;243:243–55.
[9] de Jager W, te Velthuis H, Prakken BJ, Kuis W, Rijkers GT. Simultaneous detection of 15 human cytokines in a single sample of stimulated peripheral blood mononuclear cells. Clin Diagn Lab Immunol 2003;10:133–9.
[10] Report from an Ad Hoc Subcommittee of the American Academy of Neurology AIDS Task Force. Research criteria for diagnosis of chronic inflammatory demyelinating polyneuropathy (CIDP). Neurology 1991;41:617–8.
[11] Hughes RAC, Newsom-Davis JM, Perkin GD, Pierce JM. Controlled trial prednisolone in acute polyneuropathy. Lancet 1978;2:750–3.
[12] Horiuchi I, Kawano Y, Yamasaki K, Minohara M, Furue M, Taniwaki T, et al. Th1 dominance in HAM/TSP and the optico-spinal form of multiple sclerosis versus Th2 dominance in mite antigen-specific IgE myelitis. J Neurol Sci 2000;172:17–24.
[13] Fossiez F, Djossou O, Chomarat P, Flores-Romo L, Ait-Yahia S, Maat C, et al. T cell interleukin-17 induces stromal cells to produce proinflammatory and hematopoietic cytokines. J Exp Med 1996;183: 2593–603.
[14] Schwarzenberger P, Huang W, Ye P, Oliver P, Manuel M, Zhang Z, et al. Requirement of endogenous stem cell factor and granulocyte-colony-stimulating factor for IL-17-mediated granulopoiesis. J Immunol 2000;164:4783–9.
[15] Aggarwal S, Gurney AL. IL-17: prototype member of an emerging cytokine family. J Leukoc Biol 2002;71:1–8.
[16] Hwang S-Y, Kim J-Y, Kim K-W, Park M-K, Moon Y, Kim W-U. IL-17 induces production of IL-6 and IL-8 in rheumatoid arthritis synovial fibroblasts via NF-κB- and PI3-kinase/Akt-dependent pathways. Arthritis Res Ther 2004;6:R120–8.
[17] Jovanovic DV, Martel-Pelletier J, Di Battista JA, Mineau F, Jolicoeur F-C, Benderdour M, et al. Stimulation of 92-kd gelatinase (matrix metalloproteinase 9) production by interleukin-17 in human monocyte/macrophages: a possible role in rheumatoid arthritis. Arthritis Rheum 2000;43:1134–44.
[18] Prause O, Bozinovski S, Anderson GP, Lindén A. Increased matrix metalloproteinase-9 concentration and activity after stimulation with interleukin-17 in mouse airways. Thorax 2004;59:313–7.
[19] Trajkovic V, Stosic-Grujicic S, Samardzic T, Markovic M, Miljkovic D, Ramic Z, et al. Interleukin-17 stimulates inducible nitric oxide synthase activation in rodent astrocytes. J Neuroimmunol 2001;119:183–91.
[20] Miljkovic D, Trajkovic V. Inducible nitric oxide synthase activation by interleukin-17. Cytokine Growth Factor Rev 2004;15:21–32.
[21] Kotake S, Udagawa N, Takahashi N, Matsuzaki K, Itoh K, Ishiyama S, et al. IL-17 in synovial fluids from patients with rheumatoid arthritis is a potent stimulator of osteoclastogenesis. J Clin Invest 1999;103:1345–52.
[22] Ziolkowska M, Koc A, Luszczykiewicz G, Ksiezopolska-Pietrzak K, Klimczak E, Chwalinska-Sadowska H, et al. High levels of IL-17 in rheumatoid arthritis patients: IL-15 triggers in vitro IL-17 production via cyclosporin A-sensitive mechanism. J Immunol 2000;164:2832–8.
[23] Dudler J, Renggli-Zulliger N, Busso N, Lotz M, So A. Effect of interleukin 17 on proteoglycan degradation in murine knee joints. Ann Rheum Dis 2000;59:529–32.
[24] Ishihara K, Hirano T. IL-6 in autoimmune disease and chronic inflammatory proliferative disease. Cytokine Growth Factor Rev 2002;13:357–68.
[25] Cross JT, Benton HP. The roles of interleukin-6 and interleukin-10 in B cell hyperactivity in systemic lupus erythematosus. Inflamm Res 1999;48:255–61.
[26] Larsen TB, Nieslsen JN, Fredholm L, Lund ED, Brandslund I, Munkholm P, et al. Platelets and anticoagulant capacity in patients with inflammatory bowel disease. Pathophysiol Haemost Thromb 2002;32:92–6.
[27] Ito H. IL-6 and Crohn's disease. Curr Drug Targets Inflamm Allergy 2003;2:125–30.
[28] Sebbag M, Parry SL, Brennan FM, Feldmann M. Cytokine stimulation of T lymphocytes regulates their capacity to induce monocyte production of tumor necrosis factor-alpha, but not interleukin-10: possible relevance to pathophysiology of rheumatoid arthritis. Eur J Immunol 1997;27:624–32.
[29] McLoughlin RM, Hurst SM, Nowell MA, Harris DA, Horiuchi S, Morgan LW, et al. Differential regulation of neutrophil-activating chemokines by IL-6 and its soluble receptor isoforms. J Immunol 2004;172:5676–83.
[30] Dahlman-Ghozlan K, Ortonne J-P, Heilborn JD, Stephansson E. Altered tissue expression pattern of cell adhesion molecules, ICAM-1, E-selectin and VCAM-1, in bullous pemphigoid during methotrexate therapy. Exp Dermatol 2004;13:65–9.
[31] Chertov O, Michiel DF, Xu L, Wang JM, Tani K, Murphy WJ, et al. Identification of defensin-1, defensin-2, and CAP37/azurocidin as T-cell chemoattractant proteins released from interleukin-8-stimulated neutrophils. J Biol Chem 1996;271:2935–40.
[32] Gesser B, Lund M, Lohse N, Vestergaard C, Matsushima K, Sindet-Pedersen S, et al. IL-8 induces T cell chemotaxis, suppresses IL-4, and up-regulates IL-8 production by $CD4^+$ T cells. J Leukoc Biol 1996;59:407–11.
[33] Morrissey PJ, Goodwin RG, Nordan RP, Anderson D, Grabstein KH, Cosman D, et al. Recombinant interleukin 7, pre-B cell growth factor, has costimulatory activity on purified mature T cells. J Exp Med 1989;169:707–16.
[34] van Roon JAG, Glaudemans CAFM, Bijlsma JWJ, Lafeber FPJG. Differentiation of naïve $CD4^+$ T cells towards T helper 2 cells is not impaired in rheumatoid arthritis patients. Arthritis Res Ther 2003; 5:R269–76.
[35] Giacalone B, D'Auria L, Bonifati C, Riccardi E, Mussi A, D'Agosto G, et al. Decreased interleukin-7 and transforming growth factor-beta1 levels in blister fluids as compared to the respective serum levels in patients with bullous pemphigoid. Opposite behavior of TNF-alpha, interleukin-4 and interleukin-10. Exp Dermatol 1998;7: 157–61.
[36] Ochi K, Kohriyama T, Higaki M, Ikeda J, Harada A, Nakamura S. Changes in serum macrophage-related factors in patients with chronic inflammatory demyelinating polyneuropathy caused by intravenous immunoglobulin therapy. J Neurol Sci 2003;208:43–50.
[37] Dalakas MC. Mechanisms of action of IVIg and therapeutic considerations in the treatment of acute and chronic demyelinating neuropathies. Neurology 2002;59:S13–21.
[38] Mathey EK, Pollard JD, Armati PJ. TNFα, IFNγ and IL-2 mRNA expression in CIDP sural nerve biopsies. J Neurol Sci 1999;163: 47–52.
[39] Misawa S, Kuwabara S, Mori M, Kawaguchi N, Yoshiyama Y, Hattori T. Serum levels of tumor necrosis factor-a in chronic inflammatory demyelinating polyneuropathy. Neurology 2001;56:666–9.
[40] Li Y-P, Pei Y-Y, Zhou Z-H, Zhang X-Y, Gu Z-H, Ding J, et al. PEGylated recombinant human tumor necrosis factor alpha:

pharmacokinetics and anti-tumor effects. Biol Pharm Bull 2001; 24:666–70.
[41] Horiuchi I, Ochi H, Murai H, Osoegawa M, Minohara M, Furuya H, et al. Th2 shift in mononeuritis multiplex and increase of Th2 cells in chronic inflammatory demyelinating polyneuropathy: an intracellular cytokine analysis. J Neurol Sci 2001;193:49–52.
[42] Raj DSC, Dominic EA, Wolfe R, Shah VO, Bankhurst A, Zager PG, et al. Coordinated increase in albumin, fibrinogen, and muscle protein synthesis during hemodialysis: role of cytokines. Am J Physiol Endocrinol Metab 2004;286:E658–64.
[43] Ertenli I, Kiraz S, Öztürk MA, Haznedaroğlu IC, Çelik İ, Çalgüneri M. Pathologic thrombopoiesis of rheumatoid arthritis. Rheumatol Int 2003;23:49–60.
[44] Anaya JM, Correa PA, Herrera M, Eskdale J, Gallagher G. Interleukin-10 (IL-10) influences autoimmune response in primary Sjögren's syndrome and is linked to IL-10 gene polymorphism. J Rheumatol 2002;29:1874–6.
[45] Zhou Y, Giscombe R, Huang D, Lefvert AK. Novel genetic association of Wegener's granulomatosis with the interleukin-10 gene. J Rheumatol 2002;29:317–20.
[46] Lard LR, van Gaalen FA, Schonkeren JJ, Pieterman EJ, Stoeken G, Vos K, et al. Association of the-2849 interleukin-10 promoter polymorphism with autoantibody production and joint destruction in rheumatoid arthritis. Arthritis Rheum 2003;48:1841–8.
[47] Li M-C, He S-H. IL-10 and its related cytokines for treatment of inflammatory bowel disease. World J Gastroenterol 2004;10:620–5.
[48] Willeke P, Schotte H, Erren M, Schlüter B, Mickholz E, Domschke W, et al. Concomitant reduction of disease activity and IL-10 secreting peripheral blood mononuclear cells during immunoadsorption in patients with active systemic lupus erythematosus. Cell Mol Biol 2002;48:323–9.
[49] Hattori N, Ichimura M, Nagamatsu M, Li M, Yamamoto K, Kumazawa K, et al. Clinicopathological features of Churg–Strauss syndrome-associated neuropathy. Brain 1999;122:427–39.

Prevention of Experimental Autoimmune Encephalomyelitis by Transfer of Embryonic Stem Cell-Derived Dendritic Cells Expressing Myelin Oligodendrocyte Glycoprotein Peptide along with TRAIL or Programmed Death-1 Ligand[1]

Shinya Hirata, Satoru Senju, Hidetake Matsuyoshi, Daiki Fukuma, Yasushi Uemura, and Yasuharu Nishimura[2]

Experimental autoimmune encephalomyelitis (EAE) is caused by activation of myelin Ag-reactive CD4$^+$ T cells. In the current study, we tested a strategy to prevent EAE by pretreatment of mice with genetically modified dendritic cells (DC) presenting myelin oligodendrocyte glycoprotein (MOG) peptide in the context of MHC class II molecules and simultaneously expressing TRAIL or Programmed Death-1 ligand (PD-L1). For genetic modification of DC, we used a recently established method to generate DC from mouse embryonic stem cells (ES cells) in vitro (ES-DC). ES cells were sequentially transfected with an expression vector for TRAIL or PD-L1 and an MHC class II-associated invariant chain-based MOG epitope-presenting vector. Subsequently, double-transfectant ES cell clones were induced to differentiate to ES-DC, which expressed the products of introduced genes. Treatment of mice with either of the double-transfectant ES-DC significantly reduced T cell response to MOG, cell infiltration into spinal cord, and the severity of MOG peptide-induced EAE. In contrast, treatment with ES-DC expressing MOG alone, irrelevant Ag (OVA) plus TRAIL, or OVA plus PD-L1, or coinjection with ES-DC expressing MOG plus ES-DC-expressing TRAIL or PD-L1 had no effect in reducing the disease severity. In contrast, immune response to irrelevant exogenous Ag (keyhole limpet hemocyanin) was not impaired by treatment with any of the genetically modified ES-DC. The double-transfectant ES-DC presenting Ag and simultaneously expressing immune-suppressive molecules may well prove to be an effective therapy for autoimmune diseases without inhibition of the immune response to irrelevant Ag. *The Journal of Immunology,* 2005, 174: 1888–1897.

Currently, corticosteroids and other immune suppressants are commonly used for treatment of subjects with autoimmune diseases. The medication with these drugs often leads to systemic immune suppression and consequent opportunistic infections. Thus, it is desirable to develop a therapeutic means to down-modulate immune responses in an Ag-specific manner without causing systemic immune suppression.

Experimental autoimmune encephalomyelitis (EAE),[3] an animal model for human multiple sclerosis, is characterized by neurological impairment resulting from demyelination in the CNS caused by myelin Ag-reactive CD4$^+$ T cells. This disease model is induced by immunization with myelin Ags such as myelin oligodendrocyte glycoprotein (MOG). In the current study, we wanted to try to prevent MOG-induced EAE by treatment of mice with genetically modified dendritic cells (DC). We generated double-transfectant DC presenting MOG peptide in the context of MHC class II molecules and simultaneously expressing molecules with T cell-suppressive property. We tested a strategy to down-modulate the immune response in an Ag-specific manner by in vivo transfer of such genetically modified DC to prevent development of the disease.

For efficient presentation of MOG peptide in the context of MHC class II molecules, we used a previously devised expression vector in which cDNA for human MHC class II-associated invariant chain (Ii) was mutated to contain antigenic peptide in the class II-associated Ii peptide (CLIP) region (1). An epitope inserted in this vector is efficiently presented in the context of coexpressed MHC class II molecules (2). Because they are molecules with a T cell-suppressive property, we tested TRAIL and Programmed Death-1 ligand (PD-L1). TRAIL, a member of the TNF superfamily, is constitutively expressed in a variety of cell types, including lymphocytes, NK cells, and neural cells (3, 4). TRAIL$^{-/-}$ mice are hypersensitive to collagen-induced arthritis and streptozotocin-induced diabetes (5). PD-L1, a ligand for PD-1 and member of the CD28/CTLA-4 family, is expressed on DC, IFN-γ-treated monocytes, activated T cells, placental trophoblasts, myocardial endothelium, and cortical thymic epithelial cells (6, 7). PD-1$^{-/-}$ mice spontaneously develop a lymphoproliferative/autoimmune disease, a lupus-like disease, arthritis, and cardiomyopathy (8, 9). Thus, abrogation of either of these two molecules make mice autoimmune prone, suggesting that these molecules play significant roles

Department of Immunogenetics, Graduate School of Medical Sciences, Kumamoto University, Kumamoto, Japan

Received for publication May 20, 2004. Accepted for publication December 8, 2004.

The costs of publication of this article were defrayed in part by the payment of page charges. This article must therefore be hereby marked *advertisement* in accordance with 18 U.S.C. Section 1734 solely to indicate this fact.

[1] This work was supported in part by Grants-in-Aid 12213111, 14370115, 14570421, and 14657082 from the Ministry of Education, Science, Technology, Sports, and Culture, Japan, and a Research Grant for Intractable Diseases from Ministry of Health, Labour and Welfare, Japan, and grants from the Tokyo Biochemical Research Foundation and Uehara Memorial Foundation, and by funding from Meiji Institute of Health Science.

[2] Address correspondence and reprint requests to Dr. Yasuharu Nishimura, Department of Immunogenetics, Graduate School of Medical Sciences, Kumamoto University, Honjo 1-1-1, Kumamoto 860-8556, Japan. E-mail address: mxnishim@gpo.kumamoto-u.ac.jp

[3] Abbreviations used in this paper: EAE, experimental autoimmune encephalomyelitis; MOG, myelin oligodendrocyte glycoprotein; DC, dendritic cell; Ii, invariant chain; CLIP, class II-associated Ii peptide; PD-L1, Programmed Death-1 ligand; ES cell, embryonic stem cell; ES-DC, ES cell-derived DC; PLP, myelin proteolipid protein; MBP, myelin basic protein; IRES, internal ribosomal entry site; PCC, pigeon cytochrome *c*; KLH, keyhole limpet hemocyanin.

0022-1767/05/$02.00

in maintaining immunological self-tolerance in physiological situations (10–18).

For introduction of multiple expression vectors into DC, we used a method for embryonic stem cell (ES cell)-mediated genetic modification of DC. Recently, we and another group established culture procedures to generate DC from mouse ES cells (2, 19). ES cell-derived DC (esDC or ES-DC) have the capacity comparable to bone marrow-derived DC to process and present protein Ags to T cells, stimulate naive T cells, and migrate to lymphoid organs in vivo (20, 21). A recent study using the method revealed the role of Notch signaling in differentiation of DC (22). For generation of genetically modified ES-DC, ES cells were transfected with expression vectors, and subsequently transfectant ES cell clones were induced to differentiate to DC, which expressed the products of introduced genes. Introduction of multiple exogenous genes by sequential transfection can readily be done with vectors bearing different selection markers (20).

In this study, we report that treatment of mice with ES-DC presenting MOG peptide in the context of MHC class II and simultaneously expressing TRAIL or PD-L1 significantly reduced the severity of EAE induced by immunization with the MOG peptide.

Materials and Methods

Mice

CBA, and C57BL/6 mice obtained from CLEA Japan or Charles River were kept under specific pathogen-free conditions. Male CBA and female C57BL/6 mice were mated to generate F_1 (CBF_1) mice, and all in vivo experiments were done using CBF_1 mice, syngeneic to TT2 ES cells. Mouse experiments met with approval by Animal Research Committee of Kumamoto University.

Peptides, protein, cell lines, and cytokines

The mouse MOG p35–55 (MEVGWYRSPFSRVVHLYRNGK), mouse myelin proteolipid protein (PLP) p190–209 (SKTSASIGSLCADARM YGVL), and mouse myelin basic protein (MBP) p35–47 (TGILDSI GRFFSG), were synthesized using the F-moc method on an automatic peptide synthesizer (PSSM8; Shimadzu) and purified using HPLC (23–25). Bovine MBP was purchased from Sigma-Aldrich. The ES cell line, TT2, derived from CBF_1 blastocysts, and the M-CSF-defective bone marrow-derived stromal cell line, OP9, were maintained, as described (2). L929, a fibroblast cell line originating from a C3H mouse was purchased from Japan Health Science Foundation (Osaka, Japan). Recombinant mouse GM-CSF was kindly provided by Kirin Brewery and was purchased from PeproTech.

Plasmid construction

Mouse *TRAIL* cDNA was prepared by RT-PCR amplification from total RNA of mouse spleen with PCR primers 5′-AACCCTCTAGACCGC CGCCACCATGCCTTCCTCAGGGGCCCTGAA-3′ and 5′-AAAGGGA TATCTTTACTGGTCATTTAGTT-3′. The design of these primers results in cloning of *TRAIL* cDNA downstream of the Kozak sequence (20). The PCR products were subcloned into a pGEM-T-Easy vector (Promega), and cDNA inserts were confirmed by sequencing analysis. cDNA for mouse *PD-L1* was kindly provided by Drs. T. Okazaki and T. Honjo (Department of Medical Chemistry, Kyoto University, Kyoto, Japan) (7). The cDNA fragments for *TRAIL* and *PD-L1* were cloned into pCAG-INeo, a mammalian expression vector driven by a CAG promoter and containing the internal ribosomal entry site (IRES)-neomycin resistance gene cassette, to generate pCAG-TRAIL-INeo or pCAG-PDL1-INeo. To generate a MOG peptide presenting vector, double-stranded oligo DNA encoding the MOG p35–55 epitope, 5′-CCGGTGATGGAAGTTGGTTGGTATCGTT CTCCATTCTCTCGTGTTGTTCATCTTTATCGTAACGGTAAG CTGCCCATGGGAGCT-3′, was inserted into the previously reported human Ii-based epitope-presenting vector, pCI30 (2). The coding region of this construct was transferred to pCAG-IPuro, an expression vector containing the CAG promoter and IRES-puromycin *N*-acetyltransferase gene cassette, to generate pCAG-MOG-IPuro. pCI-PCC is a pigeon cytochrome *c* (PCC) epitope-presenting vector derived from pCI30 (2).

Transfection of ES cells and differentiation of DC from ES cells

Transfection of ES cells and induction of differentiation of ES cells into DC were done as described (2, 20), with some minor modification as follows. The differentiating cells were transferred from OP9 to bacteriological petri dishes without feeder cells on day 10, and cultured in RPMI 1640 medium supplemented with 12% FCS, GM-CSF (500 U/ml), and 2-ME. The floating or loosely adherent cells were recovered from dishes by pipetting on days 17–19 and used for experiments.

RT-PCR to detect transgene products

Total cellular RNA was extracted using a SV Total RNA Isolation kit (Promega). All RNA samples were treated with RNase-free DNase I before reverse transcription to eliminate any contaminating genomic DNA. RT-PCR was done as described (20). The relative quantity of cDNA in each sample was first normalized by PCR for GAPDH. The primer sequences were as follows: *hCD74* (Ii), 5′-CTGACTGACCGCGTTACTCCCACA-3′ and 5′-TTCAGGGGGTCAGCATTCTGGAGC-3′; *TRAIL*, 5′-CTGACTGAC CGCGTTACTCCCACA-3′ and 5′-GAAATGGTGTCCTGAAAGGTTC-3′; *PD-L1*, 5′-CTGACTGACCGCGTTACTCCCACA-3′ and 5′-GCTTGTAG TCCGCACCACCGTAG-3′; and *GAPDH*, 5′-GGAAAGCTGTG GCGTGATG-3′ and 5′-CTGTTGCTGTAGCCGTATTC-3′. The sense-strand primer used for detection of transgene-derived mRNA was corresponding to the 5′ untranslated region included in the vector DNA. PCR products were visualized by ethidium bromide staining after separation over a 2% agarose gel. In one experiment, the level of expression of mRNA for *TGF-β* was detected by RT-PCR. The primer sequences were 5′-ACCATGCCAACTTCTGTCTG-3′ and 5′-CGGGTTGTGTTGGT TGTAGA-3′.

Flow-cytometric analysis

Staining of cells and analysis on a flow cytometer (FACScan; BD Biosciences) was done as described (2). Abs and reagent used for staining were as follows: anti-I-A^b (clone 3JP; mouse IgG2a), R-PE-conjugated-anti-mouse CD11c (clone N148; hamster IgG; Chemicon), R-PE-conjugated anti-mouse CD86 (clone RMMP-2; rat IgG2a; Caltag), FITC-conjugated anti-human CD74 (clone M-B741; mouse IgG2a; BD Pharmingen), FITC-conjugated goat anti-mouse Ig (BD Pharmingen), mouse IgG2a control (clone G155-178; BD Pharmingen), FITC-conjugated mouse IgG2a control (clone G155-178; BD Pharmingen), R-PE-conjugated hamster IgG control (Immunotech), R-PE-conjugated rat IgG2a control (clone LO-DNP-16; Caltag), biotinylated anti-mouse TRAIL (clone N2B2; rat IgG2a; eBioscience), anti-mouse PD-L1 (clone MIH5; rat IgG2a; eBioscience), rat IgG2a (Caltag), biotinylated rat IgG2a (eBioscience), FITC-conjugated anti-rat Ig (BD Pharmingen), and PE conjugated-streptavidin (Molecular Probes; Invitrogen Life Technologies). In some experiments, the DC fraction was gated by forward and side scatters. For detection of apoptosis of splenic $CD4^+$ T cell, Annexin V^{FITC} apoptosis detection kits (BioVision) were used. In brief, spleen cells isolated from mice treated with ES-DC were incubated with FITC-conjugated annexin V and R-PE-conjugated anti-mouse CD4 mAb (clone L3T4; BD Pharmingen), and subsequently analyzed by flow cytometry.

Cytotoxicity assay and proliferation assay of T cells stimulated with anti-CD3 mAb

Standard ^{51}Cr release assay was done as described (4). For proliferation assay of T cells stimulated with anti-CD3 mAb, splenic mononuclear cells were prepared from unprimed CBF_1 mice, and T cells were purified using nylon wool columns. X-ray-irradiated (35 Gy) ES-DC (2×10^4) and the T cells (1×10^5) were seeded into wells of 96-well flat-bottom culture plates precoated with anti-CD3 mAb (145-2C11; eBioscience) and cultured for 4 days. [^{3}H]Thymidine (6.7 Ci/mmol) was added to the culture (1 μCi/well) in the last 16 h. At the end of culture, cells were harvested onto glass fiber filters (Wallac), and the incorporation of [^{3}H]thymidine was measured using scintillation counting. For blocking experiments, anti-TRAIL (clone N2B2) or anti-PD-L1 (clone MIH5) blocking mAb (5 μg/ml) was added to the culture.

Analysis of presentation of MOG epitope by genetically modified ES-DC

MOG epitope-reactive T cells were prepared from inguinal lymph nodes of mice immunized according to protocol for EAE induction described below, using nylon wool columns. X-ray-irradiated (35 Gy) ES-DC as stimulator cells (2×10^4) were cocultured with the MOG-reactive T cells ($1.5–2 \times 10^5$) in wells of 96-well culture plates for 3 days. Proliferation of T cells in

the last 12 h of the culture was quantified based on [^{3}H]thymidine uptake, as described above.

Induction of EAE and treatment with ES-DC

For EAE induction by synthetic peptides or purified protein, 6- to 8-wk-old female CBF_1 mice were immunized by giving a s.c. injection at the base of the tail with a 0.2-ml IFA/PBS solution containing 600 μg of MOG p35–55 peptide and 400 μg of *Mycobacterium tuberculosis* H37Ra (Difco Laboratories) on day 0. In addition, 500 ng of purified *Bordetella pertussis* toxin (Calbiochem) were injected i.p. on days 0 and 2. For EAE induction by ES-DC presenting MOG peptide, ES-DC were injected at the base of the tail of mice (5×10^5 cells/mouse) at day 0, and the mice were given i.p. 500 ng of *B. pertussis* toxin in 0.2 ml of PBS on days 0 and 2. For prevention of EAE, mice were injected i.p. with ES-DC (1×10^6 cells/mouse/injection) on days −8, −5, and −2 (preimmunization treatment), or on days 5, 9, and 13 (postimmunization treatment). The mice were observed over a period of 42 days for clinical signs, and scores were assigned based on the following scale: 0, normal; 1, weakness of the tail and/or paralysis of the distal half of the tail; 2, loss of tail tonicity and abnormal gait; 3, partial hindlimb paralysis; 4, complete hindlimb paralysis; 5, forelimb paralysis or moribundity; 6, death.

Immunohistochemical analysis

Freshly excised spinal cords were immediately frozen and embedded in Tissue-Tek OCT compound (Sakura Finetechnical). Immunohistochemical staining of CD4, CD8, and Mac-1 was done, as described (20), but with some modification. In brief, serial 7-μm sections were made using cryostat and underwent immunochemical staining with mAbs specific to CD4 (clone L3T4; BD Pharmingen), CD8 (clone Ly-2; BD Pharmingen), or Mac-1 (clone M1/70; eBioscience), and N-Histofine Simple Stain Mouse MAX PO (Nichirei). Frozen sections of spleen were subjected to TUNEL staining by using ApopTag Fluorescein In Situ Apoptosis Detection kits (Serologicals). In brief, sections were incubated with digoxigenin-conjugated nucleotides and TdT, and subsequently with peroxidase-conjugated anti-digoxigenin Ab. The staining signals were developed using diaminobenzidene.

Analysis of T cell response to MOG or keyhole limpet hemocyanin (KLH)

Immunization of mice and restimulation of draining lymph node cells in vitro were done as described (26), but with some modification. In brief, ES-DC-treated and control mice were immunized at the base of the tail with MOG peptide, according to protocol for EAE induction, or 50 μg of KLH protein (Sigma-Aldrich) emulsified in CFA. After indicated days, inguinal lymph node cells and spleen cells were isolated and cultured (5×10^5 cells/well) in the presence of MOG peptide (0, 8, 2.5, or 80 μg/ml) or KLH (16, 50, or 160 μg/ml) in 10% horse serum/RPMI 1640/2-ME or 2% mouse serum/DMEM/2-ME/insulin-transferrin-selenium-X (Invitrogen Life Technologies), and the proliferative response was quantified based on [^{3}H]thymidine uptake, as described above. In addition, when mice were immunized with ES-DC expressing MOG peptide for EAE induction, spleen cells were isolated at day 14, and cultured (5×10^5 cells/well) in the presence of MOG peptide in 10% horse serum/RPMI 1640/2-ME, and the proliferative response was quantified based on [^{3}H]thymidine uptake, as described above. To analyze production of cytokines of spleen cells isolated from mice treated with ES-DC, isolated spleen cells were stimulated with 10 μM MOG peptide or irrelevant OVA peptide in vitro. After 72 or 96 h, cell supernatants were harvested and measured for cytokine content using ELISA kits (eBioscience) for IL-4, IL-10, and IFN-γ.

Statistical analysis

Two-tailed Student's *t* test was used to determine the statistical significance of differences. A value of $p < 0.05$ was considered significant.

Results

Induction of EAE in CBF_1 mice

To date, we found no study that EAE had been induced in CBF_1 mice. Therefore, before the study on therapeutic intervention, it was necessary to set up an experimental condition under which we could reproducibly induce EAE in CBF_1 mice. We compared several induction protocols using protein or peptide Ag of MOG, MBP, and PLP. As a result, we found that, when mice were s.c. injected at the base of the tail with a 0.2-ml IFA/PBS solution containing 600 μg of MOG p35–55 and 400 μg of *M. tuberculosis* accompanying an i.p. injection of 500 ng of purified *B. pertussis* toxin on days 0 and 2, EAE is reproducibly induced in CBF_1 mice with an average peak clinical score of 3.3 (Table I). We decided to use this protocol in the following experiments. In addition, inoculation of MBP p35–47, MBP whole protein, or PLP p190–209 together with *M. tuberculosis* and *B. pertussis* toxin also induced EAE in CBF_1 mice with a peak clinical score ranging between 2 and 3 (Table I).

Genetic modification of ES-DC to express MOG peptide along with TRAIL or PD-L1

At the first step in the generation of ES-DC presenting MOG peptide and simultaneously expressing TRAIL or PD-L1, TT2 ES cells were transfected with an expression vector for TRAIL (pCAG-TRAIL-INeo) or PD-L1 (pCAG-PDL1-INeo), as shown in Fig. 1*A*. Then, ES cell clones introduced with either of the expression vectors and parental TT2 ES cells were transfected with the MOG peptide expression vector, pCAG-MOG-IPuro (Fig. 1*B*). In this vector, a cDNA for human Ii was mutated to contain an oligo DNA encoding MOG p35–55 epitope in the CLIP region (1, 2, 27, 28). Resultant single- or double-transfectant ES cell clones were subjected to differentiation to ES-DC. ES-DC expressing MOG peptide, MOG peptide plus TRAIL, and MOG peptide plus PD-L1 were designated as ES-DC-MOG, ES-DC-TRAIL/MOG, and ES-DC-PDL1/MOG, respectively. The expression of mutant human Ii

Table I. *EAE induction in CBF_1 mice*[a]

Expt.	Ag	Ag Dose (μg)	Disease Incidence	Day of Onset	Mean Peak Clinical Score
1	MOG p35–55	200 × 2[b]	1/2	9.0 ± 0	1.5 ± 0
2		400	2/2	11.0 ± 0	4.0 ± 0
3		600	44/44	10.2 ± 1.3	3.3 ± 0.5
4		800	2/2	8.0 ± 0	3.0 ± 0
5	MBP p35–47	200 × 2[b]	0/2		
6		600	8/8	5.5 ± 1.3	3.0 ± 0
7	MBP protein	200 × 2[b]	0/2		
8		600	6/6	9.7 ± 1.8	3.0 ± 0
9	PLP p190–209	200 × 2[b]	0/2		
10		600	2/2	5.0 ± 0	2.0 ± 0

[a] Data are combined from a total of 21 experiments. EAE was induced by S.C. injection at the tail base of a 0.2-ml IFA/PBS solution containing 400 μg of *M. tuberculosis* and indicated peptide or MBP protein once (on day 0) or [b] twice (on days 0 and 7), together with i.p. injections of 500 ng of purified *B. pertussis* toxin on days 0 and 2.

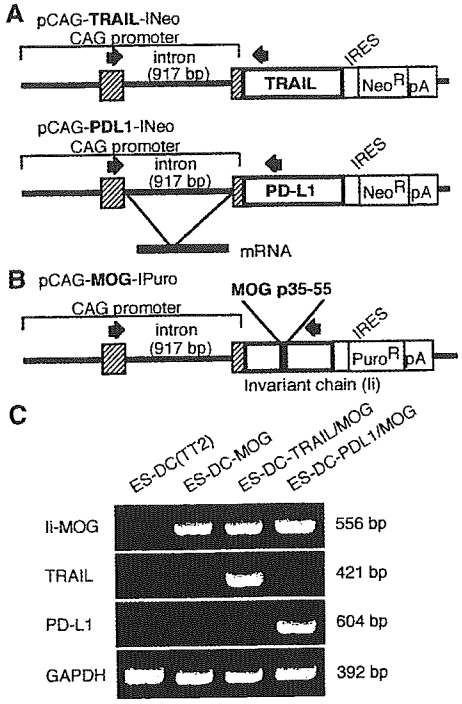

FIGURE 1. Genetic modification of ES-DC to express TRAIL, PD-L1, and Ii-MOG. *A*, The structures of pCAG-TRAIL-INeo and pCAG-PDL1-INeo, the expression vectors for TRAIL and PD-L1, and PCR primers for RT-PCR to detect transgene products are shown. Primer pairs (arrows) were designed to span the intron (917 bp) in the CAG promoter sequence to distinguish PCR products of mRNA origin (421 and 604 bp, respectively) from genome-integrated vector DNA origin. Hatched boxes indicate 5′-untranslated region of the rabbit β-actin gene included in the CAG promoter. The vectors are driven by CAG promoter (pCAG), and cDNA for TRAIL or PD-L1 are followed by the IRES-neomycin-resistance gene (Neo^R)-polyadenylation signal sequence (pA). *B*, The structure of pCAG-MOG-IPuro, the expression vector for mutant human Ii bearing MOG peptide at the CLIP region, are shown as in *A*. Primer pairs (arrows) were designed to generate PCR product of 556 bp originating from transgene-derived mRNA for CAG-MOG. *C*, RT-PCR analysis detected expression of transgene-derived mutant human *Ii* containing the MOG peptide (*Ii-MOG*), *TRAIL*, *PD-L1*, and *GAPDH* (control) mRNA in transfectant ES-DC.

containing the MOG peptide, TRAIL, and PD-L1 in ES-DC was confirmed by RT-PCR (Fig. 1*C*) and flow-cytometric analysis (Fig. 2). The mutant human Ii containing the MOG peptide was detected by intracellular staining with anti-human CD74 (Ii) mAb (Fig. 2).

ES-DC of similar morphology were generated from any of the transfectant ES cells. As shown in Fig. 2, no significant difference was observed in the level of surface expression of CD86, I-A^b, or CD11c among ES-DC derived from parental TT2 ES cells, ES-DC-MOG, ES-DC-TRAIL/MOG, and ES-DC-PDL1/MOG. Thus, forced expression of TRAIL, PD-L1, or mutant human Ii has little influence on the differentiation of ES-DC.

Functional expression of transgene-derived TRAIL and PD-L1 in ES-DC

The functional activity of TRAIL expressed in ES-DC was analyzed according to the cytotoxicity against TRAIL-sensitive L929 cells. As shown in Fig. 3*A*, ES-DC-TRAIL showed manifest killing activity against L929. In contrast, neither ES-DC (TT2) (parental TT2-derived) nor ES-DC-OVA (OVA-transfected TT2-derived ES-DC) did so. In addition, ES-DC-TRAIL inhibited the proliferation of splenic T cells stimulated with plate-coated anti-CD3 mAb (Fig. 3*B*). PD-L1 expressed on ES-DC also inhibited proliferation of splenic T cells stimulated with anti-CD3 mAb. Inhibition of anti-CD3-induced proliferation of T cells by the TRAIL and PD-L1 was abrogated by addition with anti-TRAIL and anti-PD-L1 blocking mAb, respectively (Fig. 3*B*), but not by isotype-matched control mAb (data not shown). These results indicate that transgene-derived TRAIL and PD-L1 expressed in ES-DC functioned to suppress response of T cells stimulated via TCR/CD3 complexes.

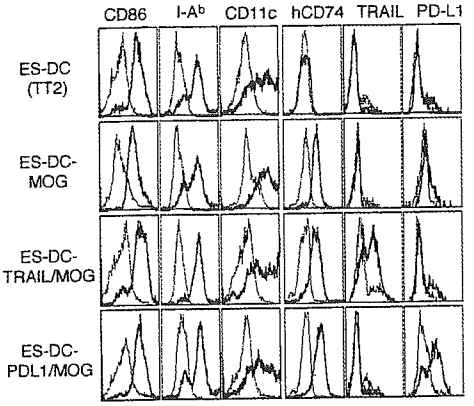

FIGURE 2. Surface phenotype of genetically modified ES-DC. Expression of cell surface CD86, I-A^b, CD11c, TRAIL, and PD-L1 on transfectant ES-DCs was analyzed by flow-cytometric analysis. Expression of mutant human Ii (hCD74) bearing MOG peptide was examined using intracellular staining. Staining patterns with specific Abs (thick line) and isotype-matched control (thin line) are shown.

Stimulation of MOG-reactive T cells by ES-DC genetically engineered to express MOG peptide

Presentation of MOG peptide in the context of MHC class II molecules by ES-DC-MOG was investigated in vitro. MOG peptide-reactive T cells were prepared from inguinal lymph nodes of mice, which developed EAE by immunization with MOG p35–55, CFA, and *B. pertussis* toxin. Proliferative response of the MOG-reactive T cells upon coculture with transfectant ES-DC was analyzed. As shown in Fig. 4*A*, ES-DC-MOG stimulated the MOG-reactive T cells to induce proliferation. In contrast, ES-DC carrying Ii-based PCC peptide expression vector (ES-DC-PCC) (2), as a control, did not do so. No proliferative response was observed when naive splenic T cells isolated from syngeneic mice were cocultured with ES-DC-MOG under the same condition (data not shown). These results indicate that the epitope-presenting vector introduced into ES-DC functioned to present the MOG peptide in the context of MHC class II molecules to stimulate MOG-specific $CD4^+$ T cells.

It has been reported that transfer of bone marrow-derived DC preloaded with MOG peptide caused development of EAE in naive mice (29, 30). We presumed that, if ES-DC-MOG could encounter with MOG-specific T cells and stimulate the T cells with MOG peptide in vivo, EAE would be developed. We injected ES-DC-MOG or ES-DC-PCC, as a control, at the base of the tail of naive mice and also gave i.p. 500 ng of *B. pertussis* toxin on the same day and 2 days later. In the results, EAE was developed in the mice transferred with ES-DC-MOG but not those transferred with ES-DC-PCC (Fig. 4*B*).

We examined whether MOG-specific T cells were activated in vivo by injection with ES-DC-MOG. Fourteen days after the injection of ES-DC and *B. pertussis* toxin, spleen cells were isolated

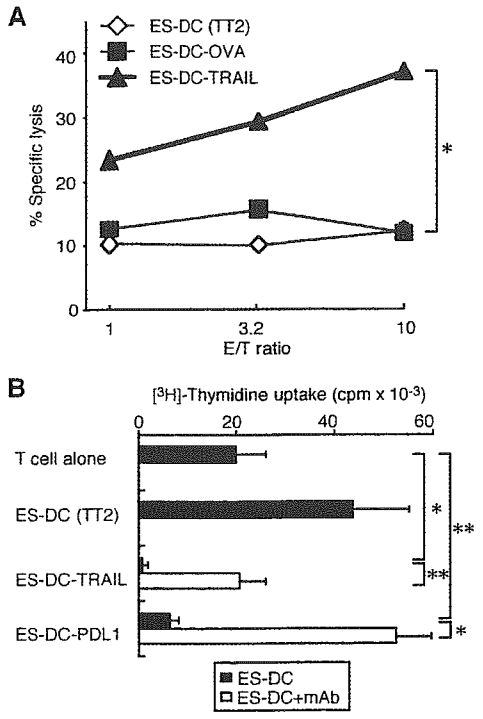

FIGURE 3. Expression of functional TRAIL or PD-L1 in ES-DC transfectants. *A*, The activity of TRAIL expressed in ES-DC was analyzed based on cytotoxicity against L929 cell. ^{51}Cr-labeled target cells (5×10^3 L929 cells) were incubated with ES-DC (TT2), ES-DC-OVA, or ES-DC-TRAIL as effector cells at the indicated E:T ratio for 12 h, and after the incubation, cytolysis of target cells was quantified by measuring radioactivity in the supernatants. Results are expressed as mean specific lysis of triplicate assays, and SDs of triplicates were <4%. *B*, Irradiated ES-DC (TT2), ES-DC-TRAIL, and ES-DC-PDL1 (2×10^4/well) were cocultured with 1×10^5 syngeneic CBF_1 splenic T cells in the presence (□) or absence (■) of blocking Ab (anti-TRAIL mAb or anti-PD-L1 mAb, 5 μg/ml) for 4 days in 96-well flat-bottom culture plates precoated with anti-CD3 mAb. Proliferation of T cells was quantified by measuring [^{3}H]thymidine incorporation. The asterisks indicate that the differences in responses are statistically significant between two values indicated by lines (*, $p < 0.01$; **, $p < 0.05$). The data are each representative of three independent and reproducible experiments with similar results.

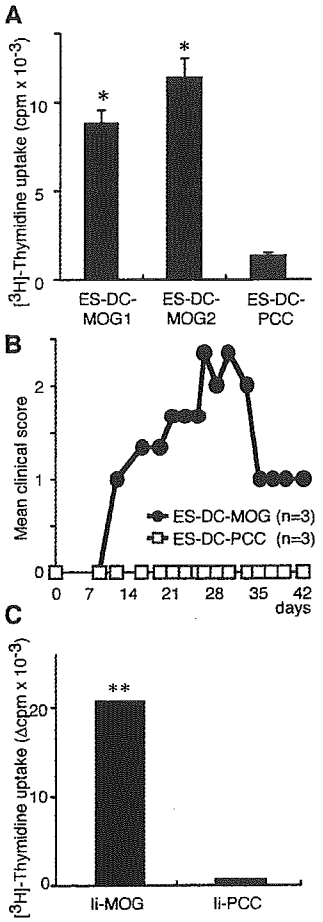

FIGURE 4. Presentation of MOG epitope by ES-DC introduced with Ii-based MOG epitope-presenting vector. *A*, T cells (1.5×10^5) isolated from inguinal lymph nodes of CBF_1 mice immunized according to the protocol for EAE induction were cocultured with one of two independent clones (2×10^4) of ES-DC-MOG or a clone of ES-DC-PCC, presenting PCC epitope, for 3 days. Proliferative response of T cells was quantified by [^{3}H]thymidine uptake in the last 12 h of the culture. *B*, CBF_1 mice (three mice per group) were injected s.c. with ES-DC-MOG or ES-DC-PCC (5×10^5) on day 0, together with i.p. injection of 500 ng of purified *B. pertussis* toxin on days 0 and 2, and the severity of induced EAE was evaluated. The disease incidence, mean day of onset ± SD, and mean peak clinical score ± SD of mice injected with ES-DC-MOG were 100%, 11.3 ± 1.7, and 2.7 ± 0.4, respectively. *C*, Spleen cells were isolated on day 14 from mice treated as in *B*, and whole spleen cells (5×10^5/well) were cultured in the presence of 1 μg/ml MOG peptide for 3 days. Proliferative response was quantified as in *A*. Data were indicated as Δcpm (value in the presence of peptide − value in the absence of peptide ($<46 \times 10^3$ cpm)), and SDs of triplicates were <9% of mean value. The asterisks indicate that the differences in responses are statistically significant compared with ES-DC-PCC (*, $p < 0.01$; **, $p < 0.05$). The data are each representative of three independent and reproducible experiments with similar results.

from the mice and cultured in the presence of MOG peptide. As shown in Fig. 4*C*, the spleen cells isolated from mice injected with ES-DC-MOG showed proliferative response to MOG peptide. In contrast, those isolated from mice injected with ES-DC-PCC did not do so. These results indicate that in vivo transferred ES-DC-MOG together with adjuvant effect of *B. pertussis* toxin stimulated MOG-specific T cells to develop EAE.

Protection from MOG-induced EAE by treatment with ES-DC expressing MOG peptide along with TRAIL or PD-L1

We examined whether TRAIL and PD-L1 expressed by ES-DC together with MOG peptide had an effect to down-modulate MOG-specific T cell responses in vitro. MOG-reactive T cells prepared as described above were cocultured with ES-DC-MOG, ES-DC-TRAIL/MOG, or ES-DC-PDL1/MOG. As shown in Fig. 5, proliferative response of the MOG-reactive T cells cocultured with ES-DC-TRAIL/MOG or ES-DC-PDL1/MOG was significantly lower than those cocultured with ES-DC-MOG, even though the three types of ES-DC expressed an almost equal level of MOG-Ii (Fig. 2). These results indicate down-modulation of the response of MOG-reactive T cells in vitro by TRAIL and PD-L1 coexpressed together with MOG peptide on ES-DC.

We tested whether or not development of EAE would be prevented by pretreatment of mice with genetically modified ES-DC. Mice were i.p. injected with ES-DC-TRAIL/MOG or ES-DC-PDL1/MOG at days −8, −5, and −2 (1×10^6 cells/mouse/injection), and sequentially immunized with MOG peptide plus adjuvants at days 0 and 2 according to the protocol described in Fig. 6*A*. As shown in Fig. 6*B* and Table II, EAE was almost